International Journal of Engineering Technologies (IJET)

Printed ISSN: 2149-0104
e-ISSN: 2149-5262

Volume: 5
No: 1
March 2019

International Journal of Engineering Technologies is an international peer–reviewed journal and published quarterly. The opinions, thoughts, postulations or proposals within the articles are but reflections of the authors and do not, in any way, represent those of the Istanbul Gelisim University.

CORRESPONDENCE and COMMUNICATION:

Istanbul Gelisim University Faculty of Engineering and Architecture
Cihangir Mah. Şehit P. Onb. Murat Şengöz Sk. No: 8
34315 Avcilar / Istanbul / TURKEY
Phone: +90 212 4227020 **Ext.** 159 or 221
Fax: +90 212 4227401
e-Mail: ijet@gelisim.edu.tr
Web site: http://ijet.gelisim.edu.tr
http://dergipark.gov.tr/ijet
Twitter: @IJETJOURNAL

Printing and binding:
Anka Matbaa
Certificate Number: 12328
Phone: +90 212 5659033 - 4800571
E-mail: ankamatbaa@gmail.com

International Journal of Engineering Technologies (IJET) is included in:

International Journal of Engineering Technologies (IJET) is harvested by the following service:

Organization	URL	Starting Date
The OpenAIRE2020 Project	https://www.openaire.eu	2015
GOOGLE SCHOLAR	https://scholar.google.com.tr/	2015
WORLDCAT	https://www.worldcat.org/	2015
IDEALONLINE	http://www.idealonline.com.tr/	2018

INTERNATIONAL JOURNAL OF ENGINEERING TECHNOLOGIES (IJET)
International Peer–Reviewed Journal
Volume 5, No 1, March 2019 - Printed ISSN: 2149-0104, e-ISSN: 2149-5262

Editorial Board

Professor Birsen YAZICI, Rensselaer Polytechnic Institute, United States

Professor Mohammad ZAMI, King Fahd University of Petroleum and Minerals, Saudi Arabia

Associate Professor Lale T. ERGENE, Istanbul Technical University, Turkey

Associate Professor Leila PARSA, Rensselaer Polytechnic Institute, United States

Associate Professor Yuichiro SHIBATA, Nagasaki University, Japan

Associate Professor Kiruba SIVASUBRAMANIAM HARAN, University of Illinois, United States

Associate Professor Yilmaz SOZER, University of Akron, United States

Associate Professor Mohammad TAHA, Rafik Hariri University (RHU), Lebanon

Assistant Professor Kyungnam KO, Jeju National University, Republic of Korea

Assistant Professor Hidenori MARUTA, Nagasaki University, Japan

Assistant Professor Hulya OBDAN, Istanbul Yildiz Technical University, Turkey

Assistant Professor Mehmet Akif SENOL, Istanbul Gelisim University, Turkey

Dr. Jorge Guillermo CALDERÓN-GUIZAR, Instituto de Investigaciones Eléctricas, Mexico

Dr. Rafael CASTELLANOS-BUSTAMANTE, Instituto de Investigaciones Eléctricas, Mexico

Dr. Guray GUVEN, Conductive Technologies Inc., United States

Dr. Tuncay KAMAS, Eskişehir Osmangazi University, Turkey

Dr. Nobumasa MATSUI, Faculty of Engineering, Nagasaki Institute of Applied Science, Nagasaki, Japan

Dr. Cristea MIRON, Politehnica University in Bucharest, Romania

Dr. Hiroyuki OSUGA, Mitsubishi Electric Corporation, Japan

Dr. Youcef SOUFI, University of Tébessa, Algeria

Dr. Hector ZELAYA, ABB Corporate Research, Sweden

From the Editor

Dear Colleagues,

On behalf of the editorial board of International Journal of Engineering Technologies (IJET), I would like to share our happiness to publish the 17th issue of IJET. My special thanks are for members of Editorial Board, Publication Board, Editorial Team, Referees, Authors and other technical staff.

Please find the 17th issue of International Journal of Engineering Technologies at http://ijet.gelisim.edu.tr or http://dergipark.gov.tr/ijet. We invite you to review the Table of Contents by visiting our web site and review articles and items of interest. IJET will continue to publish high level scientific research papers in the field of Engineering Technologies as an international peer-reviewed scientific and academic journal of Istanbul Gelisim University.

Thanks for your continuing interest in our work,

Professor Mustafa BAYRAM
Istanbul Gelisim University
mbayram@gelisim.edu.tr

---

http://ijet.gelisim.edu.tr
http://dergipark.gov.tr/ijet
Printed ISSN: 2149-0104
e-ISSN: 2149-5262


International Journal of
Engineering Technologies
IJET

Table of Contents

International Journal of Engineering Technologies, IJET

e-Mail: ijet@gelisim.edu.tr
Web site: http://ijet.gelisim.edu.tr
http://dergipark.gov.tr/ijet
Twitter: @IJETJOURNAL

Handwritten Character Recognition by using Convolutional Deep Neural Network; Review

Baki Koyuncu*, Hakan Koyuncu**

*Electrical & Electronic Engineering Dept., Faculty of Engineering and Architecture, Istanbul Gelisim University

** Computer Engineering Dept., Faculty of Engineering and Architecture, Istanbul Gelisim University

‡ Baki Koyuncu;

bkoyuncu@gelisim.edu.tr

Received: 18.02.2019 Accepted: 23.03.2019

Abstract - Handwritten character recognition is an important domain of research with implementation in varied fields. Past and recent works in this field focus on diverse languages to utilize the character recognition in automated data-entry applications. Studies in Deep Neural Network recognize the individual characters in the form of images. The reliance of each recognition, which is provided by the neural network as part of the ranking result, is one of the things used to customize the implementation to the request of the client. Convolutional deep neural network model is reviewed to recognize the handwritten characters in this study. This model, initially, learned a useful set of admittance by using local receptive areas and densely connected network layers are employed for the discernment task.

Keywords Handwritten Character Recognition, Deep Neural Network (DNN), Deep Convolutional Neural Network (DCNN).

1. Introduction

Manually handwritten character recognition is an area of research in computer vision, image contrast and style recognition. An ordinary computer achieves an ability to distinguish the characters on paper records, photographs, touch screen gadgets from different sources and converts them into machine-encoded characters. Computer application of character recognition assists in optical character reception and helps to develop frameworks of character management [1]. Picture rating is one of the symbolic issues with computers in which input pictures ought to be sent to a mark from a steady arrangement of gathering dependent pictures. In optical character recognition, (OCR), a calculation is carried out on a dataset of realized characters with the end goal of how to group the characters incorporated into the test set [2].

Previously, arrangement of calculations has been produced for characterizing letters or digits. Many of the advanced calculations in this field are brought together by digit recognition [3]. At the beginning of OCR, format coordinating and basic calculations are utilized prominently. In these calculations, the models for acknowledgment issue is made by averaging a couple of tests of letters and digits. In a considerable measure of tests, these calculations were so easy to digest the distinctive types with everything being equal would produce poor outcomes for OCR issues.

Since late 80's with the end goal of deploying larger datasets and arrangement strategies, neural network systems were utilized prevalently for recognition issues [4]. A large portion of these frameworks these days employs machine learning techniques such as neural network systems for manually handwritten character recognition (HCR). Neural systems are learning methods connected to character recognition in machine learning. Their motivation is to copy the learning task that occurs in a creature or human neural network. Being a standout amongst the most ground-breaking learning models, neural networks are valuable in mechanization of missions where the goals of an individual takes too long or is not in exact nature. A neural system can be quick at finding results and may reveal associations between observed occasions of information that humans cannot see [5].

A neural system can be deployed such as a Deep Neural Network (DNN), which utilizes in excess of one concealed layer. The contrast between neural system and deep neural system is on the depth or the quantity of concealed layers used in the system. Deep Neural Network can be a feed

forward neural system which has more than one hidden layers as shown in Fig. 1 [6].

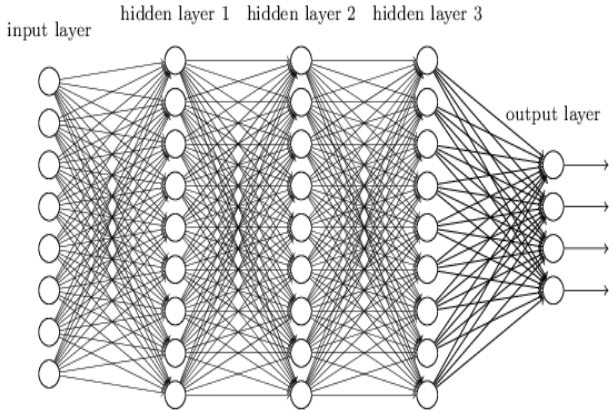

Fig. 1. Architecture of DNN [6].

DNN comprises of input layer, output layer and various intermediate layers. Hence, the quantity of associations and trainable components are very large. The deep neural system requires substantial gathering of examples to hinder over fitting and numerous regular signs have compositional arrangements [7]. In images, nearby arrangements of edges create frame themes, themes gather into parts and parts shape subjects. Comparable advances exist from sounds as well such as phonemes, syllables, words and sentences.

The pooling enables a summary of data to shift to next layers when data in the previous layer change in position and appearance. One class of Deep Neural System with generally smaller arrangement of components and simple to prepare is called Convolutional Neural System (CNN) [8][9]. CNN is an organic disclosure of multilayer perceptron (MLP). A multilayer neural network system was proposed by Fukushima, [10], and has employed manually written character recognition and other computer vision issues. LeCun [11], has utilized Convolutional Neural Network system to sort out the ImageNet dataset.

Current developments on CNN has been focused on computer vision issues such as picture division [12], picture inscribing [13] and picture grouping [14]. There has been a considerable measure of interest about manually written character digits [15] and recognition of characters in different dialects. This interest has grown due to the plausible perplexity and likeness of written characters by hand and generosity in classes.

In this study, hand written characters will be analyzed and character recognition is reviewed by utilizing, initially, DNN and later on CNN techniques. This paper organizes as follows. In Section I, the introduction and literature review is given. In Section II, related work is summarized. In Section III, CNN technique is explained and all the related models are described. Distinctive kinds of layers in CNN such as input layer, hidden layers output layer is explained in this section. In Section IV, general conclusion is given.

2. Alternative Techniques

Many researchers have developed systems for handwritten character recognition. Several important systems are mentioned in this work. Character recognition frameworks have been engineered utilizing different rationale [16]. The framework developed by some researches can be constructed by using hardware with very large scale integration circuitry (VLSI). The input character recognition of this framework is resistant to dynamic motion. Other researches utilized hamming error correcting codes from communication theory with neural network system in their framework. Another technique was developed to acknowledge the written hand characters in different dialects in its' Neural network System [17]. These frameworks generated accurate results but also made mistakes if the written hand characters are in extreme format. One of the researchers has even offered a strategy to relate the dependence between hand writers and their penmanship [18]. These studies have mostly utilized the Multi-layer feed forward neural network system in their methods.

3. Reviewed Techniques

Convolutional Neural Network Technique is basically neural network systems that utilize convolution instead of general network systems with similar number of layers. It has wide applications in fields like picture and video acknowledgment, characteristic dialect handling and recommended frameworks. From design perspective, CNN is a neural network system that utilizes no less than one convolution process in no less than one of its layers. The convolution procedure is carried out in convolution layer. There are three fundamental process that must exist in convolution layer. These are convolution, sub sampling/pooling, and actuation. A CNN incorporates a heap of convolution layer and a maximum pooling layer pursued by a complete actuation layer. The convolution layer is the most critical layer of system. It does the convolution task. The pooling layer comes after the convolution layer. This layer is essential on the grounds that if there should be an occurrence of bigger pictures, the quantity of trainable components can be exceptionally large. This expands the time taken to prepare a neural network system and this is not practical. The pooling layer is utilized to reduce the span of picture.

In this study, Modified National Institute of Standards and Technology (MNIST) database published by US department of commerce is deployed. This database contains a huge number of pictures of written hand characters. Reducing the size of the pictures reduces the general time taken to prepare the neural network system to operate. Fig. 2 shows the general view of layers present in CNN. The first layer is input layer, second layer is convolutional layer, intermediate layers are pooling layers (subsampling) and convolutional layers. Last two layers of the network are the fully connected layer and output layer.

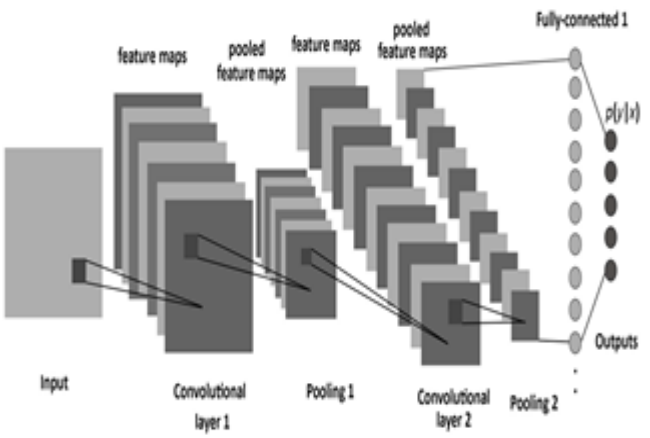

Fig. 2. Architecture of CNN [15]

A. Input Layer

The input layer is the layer of initial image which contributes to the operation at the front of the system architecture and the input is the character image as shown in Fig. 3. The input layer can be a gray scale or an RGB image. The input layer can have dimensions WxHxD where WxH is the width and height of the image and D is the depth of the image. Depth is 1 pixel for grayscale and 3 pixels for RGB images. Thus, the input layer for RGB image has dimensions 32x32x3 as seen in Fig. 3a and for Gray scale image has dimensions 32x32x1 as seen in Fig. 3b.

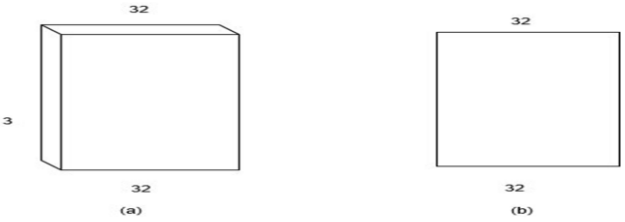

Fig. 3. Input images

B. Convolution Layer

This is the block structure after the input layer as seen in Fig. 2 where most of the computational work is done. The convolutional layer comprises of channels with learning capabilities and called components of this layer. Each channel is identified as a filter. This filter is a square matrix of spatial width and length in pixels with a depth. These channels, hence the filters, cover the full information volume. A model channel in convolutional layer can have a size of 5x5x3 pixels where 5 pixels' width, length and 3 pixels' depth. These channels are identified as shaded channels and the images used are RGB images. In this study, filters will have depth of 1 pixel and a size of 5x5x1 pixels and the character images employed are non-colored images.

During the forward pass of the neural network operation, each channel is sided widthwise and lengthwise with other channels creating a 2 dimensional information volume. Pixel intensity information of the character shapes are considered across the channels and other areas in the channels are shown as 0 pixels. As each channel is crossed through channel cross section with a width and length of the information volume, a 2-dimensional partial character outline is delivered from each channel which gives the response of that channel at each image local position.

Instinctively, the filter section is convolved over the entire image and the generated output after convolution are called initial maps as shown in Fig. 4.

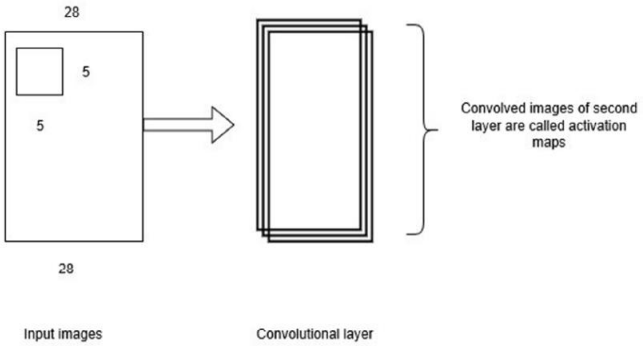

Fig. 4. Activation maps of second layer

These initial maps are called activation maps of 2nd convolutional layer. Size and number of filters depend on the experimental conditions There is no well-defined procedure to identify them. Initially, filters can contain small number of random values. But they are learnable parameters and their values will be updated with each learning stage of the network. The input layer accepts the image with dimensions WxHxD. Additional two hyper parameters such as Filter size (F) and stride (S) are deployed during convolution operation in order to generate an input for another layer with dimensions $W_1xH_1xD_1$.

W_1 and H_1 are given by equations (1) and (2). Depth D_1 remains same as D. In these equations P is called padding. It introduces new row and column of zeros on each side of image.

$$W_1 = (F - W + P)/(S + 1) \qquad (1)$$

$$H_1 = (F - H + P)/S + 1) \qquad (2)$$

In this study, 32 filters were employed each with a size of 5x5x1, P=1, and S=0. Thus, the dimensions of second layer image become 32(28x28).

C. Pooling Layer

The location of Pooling layers is between convolutional layers in a convolutional architecture. Pooling layers reduce the quantity of components when the images are excessively large and also control overfitting. Additionally, local pooling called sub testing or down inspecting is introduced in this layer to eliminate the unused elements of each image and to keep the critical data. The Pooling Layer works freely on the information section at

each depth and changes information at spatial dimensions. There are several types of spatial pooling. These are Maximum Pooling (MAX), Normal Pooling and Whole Pooling. MAX pooling is the most commonly used pooling. It has a pooling layer with channels of size 2x2 utilized with a stage of 2 down-inspecting local pooling. Each Maximum pooling task selects a maximum value from 4 numbers. The depth dimension stays constant. In this study, maximum filter size of 3x3, P=1 and S= 2 are deployed in first pooling layer. The output dimensions of this layer become 32(14x14). Different filters can also be employed in pooling layer.

D. Fully connected Layer

The layer identified as FC layer is the last layer of the neural network system. The image matrix arriving from pooling layer 2 with W and H dimensions are converted into 1 dimensional vector form and applied into network system. See Fig. 2. The introduction of this layer can thus improve the framework enlargement pursued by a tendency to balance. There can be multiple fully connected layers depending upon the application architecture. In this study, it is assumed that, there are 41 character classes; hence the output layer has 41 neurons. The fully connected layer has 256 neurons. The neuron number in this layer is chosen experimentally. Fig. 5 displays the complete architecture used in this study. Matlab Neural network toolbox is used in the experiments.

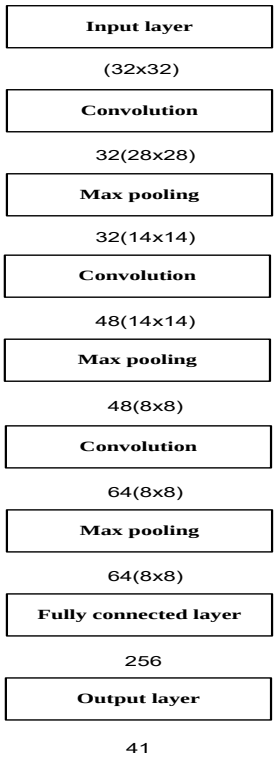

Fig. 5. CNN architecture used in this study.

4. Conclusion

A convolutional neural system is reviewed for readers' attention. This system is extremely dynamic for perceiving written hand characters. This work depends on the reception of characters at the input of (CNN). Contrast with other deep learning architectures, CNN has preferable execution in both images and big data. The aim to use deep learning was to take advantages of the power of CNN that are able to administer large dimensions of input and share their weights. The CNN architecture has thousands of elements and hyper-elements to tune. It is not clear why convolutional networks are prosperous when general back-propagation algorithms fail. It may simply be that convolutional networks work in hierarchy and solve complex framework by simpler ones.

Acknowledgements

The authors appreciated the assistance received from engineering faculty of Istanbul Gelisim University and MSc student Ali H. Abdulwahhab for his contributions in the study.

References

[1] R. Vaidya, D. Trivedi, S. Satra, M. Pimpale, "Handwritten Character Recognition Using Deep-Learning". Second International Conference on Inventive Communication and Computational Technologies (ICICCT), pp. 772-775, 2018

[2] G. S. Budhi and R. Adipranata, "Handwritten Javanese Character Recognition Using Several Artificial Neural Network Methods", J.ICT Res. Appl., vol. 8, no. 3, pp. 195–212, 2015

[3] A. Rajavelu, M.T. Musavi, and M.V. Shirvaikar, "A neural network approach to character recognition", *Neural Netw.*, vol. 2, no. 5, pp. 387– 393, 1989.

[4] S. Mori, C. Y. Suen, and K. Yamamoto, "Historical review of OCR research and development," Proc. IEEE, vol. 80, no. 7, pp. 1029 –1058, 1992

[5] J. Pradeep, E. Srinivasan and S. Himavathi. "Neural Network based Handwritten Character Recognition system without feature extraction", International Conference on Computer, Communication and Electrical Technology ICCCET 2011

[6] K. Gurney, "An introduction to neural networks", UCL Press, 1997

[7] Y. LeCun, Y. Bengio and G. Hinton, "Deep learning", Nature, Vol. 521, pp. 436-444, 2015

[8] Y. Liang, J. Wang, S. Zhou, Y. Gong, and N. Zheng, "Incorporating image priors with deep convolutional neural networks for image super resolution", Neurocomputing, Vol. 194, pp. 340- 347, 2016

[9] R. Nijhawan, H. Sharma, H. Sahni, and A. Batra, "A deep learning hybrid CNN framework approach for vegetation cover mapping using deep features", 13th International Conference on Signal Image Technology & Internet-Based Systems (SITIS), pp. 192-196, 2017

[10] K. Fukushima, "Neocognitron: A self-organizing neural network model for a mechanism of pattern recognition

unaffected by shift in position", Biological Cybernetics., vol. 36, no. 4, pp. 193–202, 1980

[11] A. Krizhevsky, I. Sutskever, and G. E. Hinton, "ImageNet classification with deep convolutional neural networks," Advances in neural information processing systems, pp. 1097–1105, 2012

[12] C. Farabet, C. Couprie, L. Najman, and Y. LeCun, "Learning hierarchical features for scene labeling", IEEE Trans. Pattern Anal. Mach. Intel., Vol. 35, no. 8, pp. 1915–1929, 2013

[13] O. Vinyals, A. Toshev, S. Bengio, and D. Ethan, "Show and tell: A neural image caption generator", Proceedings of the IEEE Conference onComputer Vision and Pattern Recognition, pp. 3156–3164, 2015

[14] D. C. Ciresan, U. Meier, J. Masci, L. Maria Gambardella, and J. Schmidhuber, "Flexible, high performance convolutional neural networks for image classification", Proceedings in 22nd International Joint Conference on Artificial Intelligence, Vol. 22, pp. 1237-1242, 2011

[15] E. Kussul and T. Baidyk, "Improved method of handwritten digit recognition tested on MNIST database", Image Vis. Compute., vol. 22, no. 12, pp. 971–981, 2004

[16] W. Lu, Z. Li, B. Shi." Handwritten Digits Recognition with Neural Networks and Fuzzy Logic", IEEE International Conference on Neural Networks, Vol. 3, pp.1389-1392, 1995

[17] P. Banumathi, G. M. Nasira, "Handwritten Tamil Character Recognition using Artificial Neural Networks", International Conference on Process Automation, Control and Computing, 2011

[18] B. V. S. Murthy," Handwriting Recognition Using Supervised Neural Networks", International Joint Conference on Neural Networks, 1999

Modeling the Shear Strength of Reinforced Aerated Concrete Slabs via Support Vector Regression

Ahmet Emin Kurtoglu*‡, Derya Bakbak**

*Department of Civil Engineering, Istanbul Gelisim University, 34315, Avcılar, Istanbul, Turkey

**The Grand National Assembly of Turkey (TBMM), 06534, Çankaya, Ankara, Turkey

(aekurtoglu@gelisim.edu.tr, derya.bakbak@tbmm.gov.tr)

‡Corresponding Author; Ahmet Emin Kurtoglu, Istanbul Gelisim University, 34315, Avcılar, Istanbul, Turkey, Tel: +90 212 422 7000,

aekurtoglu@gelisim.edu.tr

Received: 02.02.2019 Accepted:02.03.2019

Abstract- Autoclaved aerated concrete (AAC) attracts attention as it provides superior material characteristics such as high thermal insulation and environmentally friendly properties. Apart from non-structural applications, AAC is being considered as a structural material thanks to its characteristics such as lighter weight compared to normal concrete, resulting in lower design costs. This study focuses on the feasibility of support vector regression (SVR) in predicting the shear resistance of reinforced AAC slabs. An experimental dataset with 271 data points extracted from eleven sources is used to develop models. Based on random selection, the dataset is divided into two portions, 75% for model development and 25% for testing the validity of the model. Two SVR model types (epsilon and *Nu*) and four kernel functions (linear, polynomial, sigmoid and radial basis) are used for model development and the results of each model and kernel type is presented in terms of correlation coefficient (R^2) and mean squared error (*MSE*). Results show that epsilon model type with radial basis function yields the best SVR model.

Keywords Autoclaved aerated concrete, reinforced concrete slab, shear strength, support vector regression, modelling.

1. Introduction

Autoclaved aerated concrete (AAC) is made of cement or lime mortar which contains air voids entrapped in the matrix by means of an expansion agent. AAC has been used in the construction industry for non-structural and structural applications since mid-1920s. The main property of AAC is high porosity, i.e., up to above 70% of the volume contains air voids, resulting in lower density which minimizes the design cost [1]. AAC is considered to be environmentally friendly material as it reduces 70% and 40% energy per material volume as compared to normal concrete and bricks, respectively. It also provides high thermal insulation [2, 3].

Production of AAC panel elements with reinforcement can offer an alternative for low-rise precast construction. 60% of new building constructions in Europe are built with different types of AAC elements [4]. In the housing industry in China, reinforced AAC materials for exterior walls are preferred to other materials [4].

Shear resistance of reinforced normal concrete or AAC slabs without shear reinforcement is a complex phenomenon. It is known that the shear resistance depends not only on the concrete properties but also on the shear-span-to-depth (a/d) ratio as well as the presence of tensile reinforcement (Fig. 1). Aroni and Cividini (1989) proposed a formulation (Eq. 1a, Eq.1b) for the shear strength of reinforced AAC slabs with a modification to the formulation available for normal concrete slabs [5]. Fig. 2 shows a typical shear resistance test setup of reinforced AAC slab.

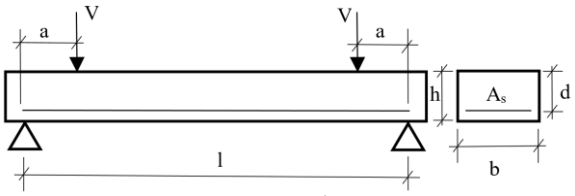

Fig. 1. Schematic of typical test setup

$$\tau_u = 0.035 f_c + 1.163\rho(d/a) - 0.053 \quad \text{within the normal range} \tag{1a}$$

$$\tau_u = 0.039 f_c + 0.82\rho(d/a) - 0.075 \quad \text{outside the normal range} \tag{1b}$$

where τ_u is the ultimate shear stress in MPa ($\tau_u = V_u/bd$), f_c is the compressive strength of AAC in MPa, ρ is reinforcement ratio ($100A_s/bd$), d is the effective depth in mm, a is the shear span in mm.

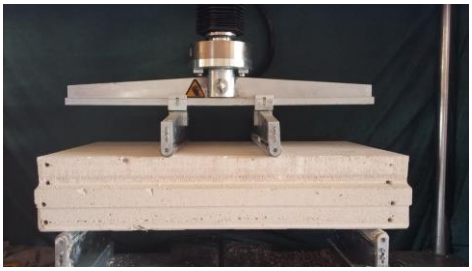

Fig. 2. Test setup

In this study, a novel machine learning based regression method, namely support vector regression, is implemented to produce predictive models for the shear resistance of reinforced AAC slabs.

2. Experimental Data

The experimental data consist of 271 data points extracted from previously published papers [6-15]. Table 1 summarizes the origins and product types for the tests. All data points were included in the modeling process. Data inputs are *fc* (compressive strength), *d/a* (span-to-depth ratio) and ρ (reinforcement ratio), the output is τ *(ultimate shear stress, V/bd).* Table 2 presents the statistical variations of input and output parameters. Some specimens contained compression reinforcement consisting of two or three bar. Possible contributions of these bars in shear strength have been neglected.

Table 1 References and types of test product

Series No.	Reference	Product type
1	Bernon [14] (France)	Siporex
2	Blaschke [13] (Germany)	Ytong
3	Briesemann [12] (Germany)	Hebel
4	Cividini [11] (Yugoslavia)	Siporex, Ytong
5	Dalby [10] (Sweden)	Siporex
6	Edgren [10] (Sweden)	Siporex
7	Kanoh ’66 [9] (Japan)	Siporex
8	Kanoh ’69 [8] (Japan)	Hebel
9	Matsamura [7] (Japan)	ALC
10	Newarthill [6] (UK)	Siporex
11	Regan [15] (UK)	Durox

Table 2 Statistics of experimental data

	fc (MPa)	*d/a*	ρ	τ_u *(Mpa)*
Minimum	2.3	0.08	0.12	0.107
Maximum	7.8	0.766	1.349	0.836
Mean	3.78	0.24	0.41	0.24
Standard deviation	1.31	0.16	0.26	0.14
Coeff. of variation	0.35	0.66	0.62	0.56

3. Support vector machines

Support vector machines (SVMs) were first identified by Boser et al. (1992) is an artificial intelligence learning technique developed to solve the classification problem [16]. However, researchers began using SVM to solve regression problems, and this method was named support vector regression (SVR).

SVM has performed well in many applications such as text analysis, face recognition, image processing and bioinformatics, as well as a strong digital basis in statistical learning theory. This shows that SVM is one of the most modern methods of machine learning and data mining, along with other methods such as neural networks and fuzzy systems [17].

2.1. Support vector regression (SVR)

In SVR, the main purpose is to obtain a function whose actual output value is estimated with the maximum deviation of epsilon and to get two parallel planes for this function. The distance between these planes must be minimized. [18].

For the training data set presented in SVR, the main objective is to find a function with the difference from specific target. At the same time, the function should be flattest with errors less than a certain amount without excess deviation [18]. The (linear) ε-insensitive loss function *L(x, y, f)* is described as

$$L^{\varepsilon}(x,y,f)=|y-f(x)|_{\varepsilon}=\begin{cases}0 & if\ |y-f(x)|\le\varepsilon\\ |y-f(x)|-\varepsilon & otherwise\end{cases} \quad (3a)$$

where *f* is a real-valued function on a *x* and the quadratic *ε*-insensitive loss is defined by

$$L_2^{\varepsilon}(x,y,f)=|y-f(x)|_{\varepsilon}^2 \quad (3b)$$

Fig. 3 demonstrates the linear and quadratic *ε*-insensitive loss function for zero and non-zero *ε*.

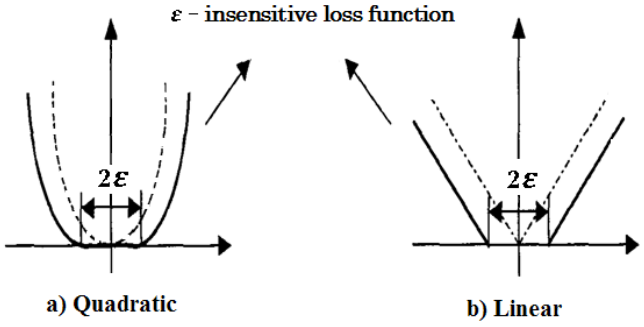

Fig. 3 The form of linear and quadratic *ε*-insensitive loss function for zero and non-zero *ε*.

The loss function defines the accuracy performance. Performing linear regression in the high-dimension feature space by the use of *ε*-insensitive loss function, SVM attempts to reduce the model complexity by performing the minimization of $\|\omega\|^2$. By introducing slack variables $\xi_j,\xi_i^* i=1,..n$

$$L(y,f(x,\omega))=|y-f(x)|_{\varepsilon}^2 \quad (3c)$$

$$L_2^{\varepsilon}(x,y,f)=|y-f(x)|_{\varepsilon}^2$$

to determine the deviation of training data outside *ε* -zone. Following formulation is implemented for the minimization of SVM regression:

$$\frac{1}{2}\|\omega\|^2+c\sum_{i=1}^{n}(\xi_{i+}\xi_i^*) \text{ subject to } \xi_j,\xi_i^* i=1,..n \quad (3d)$$

$$\xi_j,\xi_i^* i=1,..n \quad (3e)$$

The solution of this optimization problem can be found by transforming it into the dual problem:

$$f(x)=\sum_{i=1}^{n_{sv}}(\alpha_j-\alpha_i^*)K(x_j,x)+b \text{ subject to } 0\le\alpha_i^*\le C, 0\le\alpha_j\le C \quad (3f)$$

where n_{sv} is the number of support vectors (SVs), a_i^* and a_j are the Lagrange multipliers and $K(x_j, x)$ is a kernel function and *b* is the bias term. The generalization of SVM depends on the appropriate settings of meta-C, ε, and kernel parameters. Available software applications generally have the option for manual specification of meta-parameters [19].

The model complexity and the degree, to which deviations larger than *ε* are tolerated, are controlled by a parameter *C* controls in optimization formulation. Parameter *ε* describes the width of *ε*-insensitive zone, which is utilized to fit the training data. Value of *ε* can affect the number of support vectors used to form the regression function. On the other hand, greater *ε*-insensitive values cause more 'flat' predictions. Although in different ways, both *C* and *ε* values affect model complexity (flatness) [19].

Several kernel functions are used in machine learning. Four functions used in this study are:

Linear function:

$$K(x_i,x)=x_i x \quad (4a)$$

Polynomial function:

$$K(x_i,x)=(x_i(x+1))^d \quad (4b)$$

Radial-based function:

$$K(x_i,x)=\exp\left[-\frac{(x_i-x)(x_i-x)}{2\sigma^2}\right] \quad (4c)$$

Sigmoid function:

$$K(x_i,x)=\tanh(x_i(x+1)) \quad (4d)$$

where x_i and *x*, are the training and test inputs, respectively, *σ* is the Gaussian kernel function and *d* is the polynomial degree of kernel function.

4. Model Development

Experimental data (three inputs and one output) is divided into two portions, i.e., 75% of the data is used as model training set, 25% is used for testing the validity of the model. SVR models are developed by optimizing the meta parameters *C* and *ε* or *Nu*, by performing a grid search along a pre-specified range. The model with best correlation coefficient (R^2) is selected for each model type and kernel function. Correlation coefficient (R^2) measure the relationship between predicted and experimental data, in

which $R^2 = 1$ means significant correlation and $R^2 = 0$ means no correlation. Eq. 5.1 and Eq. 5.2 are used for calculating correlation coefficient (R^2) and mean squared error (*MSE*), respectively. Fig. 4 shows the correlation coefficient (R^2) values for eight SVR models developed using two model types and four kernel functions. SVR models developed with Radial Basis kernel appear to yield better fitting results as compared to other kernel types. Epsilon model type with radial basis kernel gives the best correlation coefficient (total set: 0.936, training set: 0.945, testing set: 0.901).

$$R^2 = 1 - \left(\frac{\sum_{i=1}^{N} (o_i - t_i)^2}{\sum_{i=1}^{N} (o_i - o')^2} \right) \tag{5.1}$$

$$MSE = \frac{\sum_{i=1}^{N} (o_i - t_i)^2}{N} \tag{5.2}$$

where o_i is the experimental value of *ith* data, t_i is the predicted value of *ith* data, N is the number of data used for training and testing of SVR models.

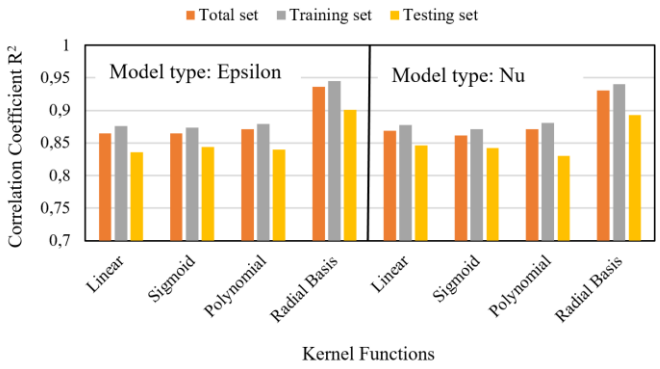

Fig. 4 Correlation coefficient of SVR models

Fig. 5 shows mean squared error (*MSE*) values calculated for each SVR model type, using Eq. 5.2. SVR models produced with sigmoid kernel appear to yield significantly large errors while models with radial basis kernel produces less *MSE*. Table A.1. lists the support vectors generated by the SVR-Eps-Rad model.

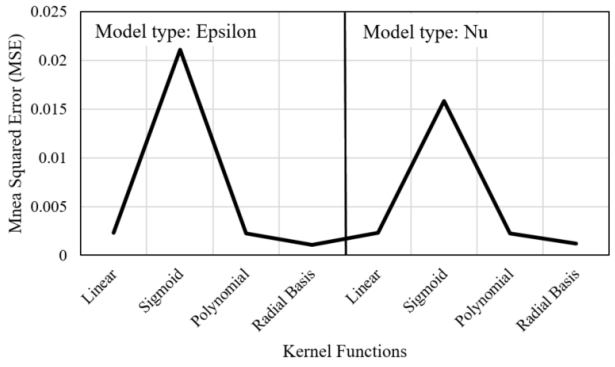

Fig. 5 Mean squared error of SVR models

Fig. 6 compares the experimental and estimated values of SVR-Eps-Rad model both for training and testing datasets.

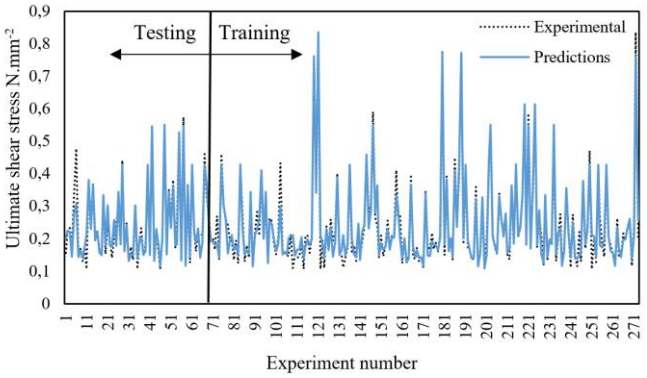

Fig. 6 Experimental data versus predictions of SVR-Eps-Rad model

According to [20], if the correlation coefficient R^2 is greater than 0.8 and the error values are at a desirable range, there is a strong correlation between predicted and real values. Regarding Fig. 7, proposed SVR-Eps-Rad model has a R^2 value of 0.931 for whole set and the error is acceptable, as seen in Fig. 5.

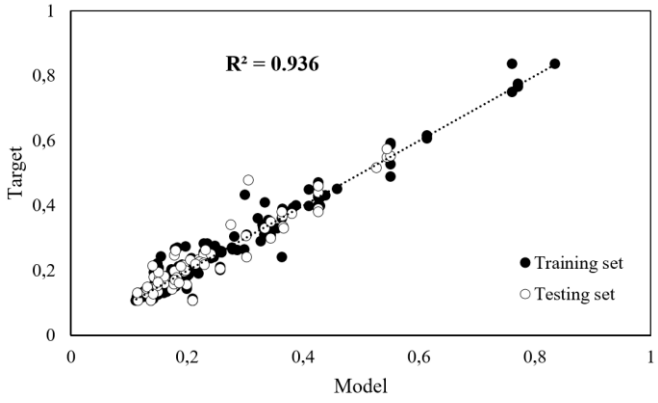

Fig. 7 Comparison of predicted values and experimental values of Ultimate Shear Stress (MPa)

5. Conclusion

This study analyzes the feasibility to use support vector regression method to propose a predictive model for ultimate shear stress of reinforced aerated concrete. Different model types (epsilon and *Nu*) and kernel function types (linear, sigmoid, polynomial, radial basis) are used for model development to analyze the feasibility. An experimental dataset with 271 data points is implemented to develop models. Dataset is divided into two portions, 75% for model development and 25% is for testing the validity of the model, based on random selection. Each model is analyzed statistically to determine the prediction performance. For this, mean squared error (*MSE*) and correlation coefficient (R^2) are used. For epsilon model type, R^2 values for total set are 0.865, 0.865, 0.871 and 0.936 for linear, sigmoid, polynomial and radial basis kernel types, respectively. On the other hand, for *Nu* model type, R^2 values for total set are 0.869, 0.862, 0.871 and 0.931 for linear, sigmoid, polynomial and radial basis kernel types, respectively. Hence, SVR model based on epsilon model type and radial basis kernel function gives the best correlation coefficient values. Sigmoid kernel based models yield largest *MSE* values while radial basis kernels produce less *MSE*. Finally, the results confirm that support vector regression (SVR) method has the advantage to be easily applied and yield reasonably accurate prediction performance.

References

[1] A. Thongtha, S. Maneewan, C. Punlek, and Y. Ungkoon, "Investigation of the compressive strength, time lags and decrement factors of AAC-lightweight concrete containing sugar sediment waste", Energy and Buildings, vol. 84, No., pp. 516-525, 2014.

[2] X. Qu and X. Zhao, "Previous and present investigations on the components, microstructure and main properties of autoclaved aerated concrete–A review", Construction and Building Materials, vol. 135, pp. 505-516, 2017.

[3] A. Bonakdar, F. Babbitt, and B. Mobasher, "Physical and mechanical characterization of fiber-reinforced aerated concrete (FRAC)", Cement and Concrete Composites, vol. 38, pp. 82-91, 2013.

[4] A. Taghipour, E. Canbay, B. Binici, A. Aldemir, U. Uzgan, and Z. Eryurtlu, "Seismic behavior of reinforced autoclaved aerated concrete wall panels", ce/papers, vol. 2, No. 4, pp. 259-265, 2018.

[5] S. Aroni and B. Cividini, "Shear strength of reinforced aerated concrete slabs", Materials and Structures, vol. 22, No. 6, pp. 443-449, 1989.

[6] N. Edgren, "Shear tests on Siporex slabs (Newarthill Factory, UK)'", unpublished report (Internationella Siporex AB, Central Laboratory, 1981–82).

[7] A. Matsumura, "Shear strength and behavior of reinforced autoclaved lightweight cellular concrete members", Trans. Architect. Inst. Jpn, vol. 343, pp. 13-23, 1984.

[8] Y. Kanoh, "Report of Hebel research'", unpublished report (Meiji University, 1969).

[9] Y. Kanoh, "Shear strength of the reinforced autoclaved lightweight concrete one-way slabs'", Proceedings of Research Papers of the Faculty of Engineering, Meiji University, vol., No. 21, 1966.

[10] N. Edgren, "Shear tests on Siporex slabs (Dalby Factory, Sweden)'", unpublished report (Internationella Siporex AB, Central Laboratory, 1979).

[11] B. Cividini, "Ispitivanje granicne nosivosti armiranih ploca od plinobetona (Investigation of bearing capacity of reinforced aerated concrete slabs)", Proceedings of 17th JUDIMK Congress, Sarajevo, October, pp. 19-41, 1982.

[12] D. Briesemann, Die schubtragfähigkeit bewehrter platten und balken aus dampfgehärtetem gasbeton anch versuchen, Ernst, 1980.

[13] R. Blaschke, "Shear load behaviour of AAC reinforced units of high compressive strength (GB 6.6)'", unpublished report (Ytong Research Laboratory, Schrobenhausen, 1988), 1988.

[14] N. Edgren, "Shear tests on Siporex slabs (Bernon Factory, France)'", unpublished report (Internationella Siporex AB, Central Laboratory, 1979–80).

[15] P. Regan, "Shear in reinforced aerated concrete", International Journal of Cement Composites and Lightweight Concrete, vol. 1, No. 2, pp. 47-61, 1979.

[16] B.E. Boser, I.M. Guyon, and V.N. Vapnik, "A training algorithm for optimal margin classifiers", Proceedings of the fifth annual workshop on Computational learning theory, pp. 144-152, 1992.

[17] L. Wang, Support Vector Machines: theory and applications, vol. 177, Springer, 2005

[18] N. Chen, W. Lu, J. Yang, and G. Li, Support vector machine in chemistry, vol. 11, World Scientific, 2004

[19] V. Cherkassky and Y. Ma, Selection of meta-parameters for support vector regression, Artificial Neural Networks—ICANN 2002, Springer, 2002, 687-693.

[20] G.N. Smith, "Probability and statistics in civil engineering", Collins Professional and Technical Books, vol. 244, No., 1986.

Appendix

Table A.1. Support vectors for SVR-Eps-Rad model

Index	Coefficient	Support Vector (normalized)
1	88888.9	-0.745455, -0.892128, -0.674532
2	88888.9	-0.62, -0.41691, -0.158666
3	88888.9	-0.527273, -0.833819, -0.563873
4	-83099.1	-1, -0.177843, -1
5	-88888.9	-0.625455, -0.810496, -0.389748
6	-79853.3	-0.745455, -0.77551, -0.558991
7	88745.5	-0.62, 0.950437, 1
8	88888.9	-0.610909, -0.909621, -0.554109
9	-88888.9	-0.659273, -0.944606, -0.485761
10	-88888.9	-0.745455, -0.723032, -0.785191
11	67164.1	-0.8, -0.6793, -0.536208
12	-88888.9	1, 0.48105, -0.728234
13	-88888.9	-0.549091, -0.795918, -0.607811
14	88888.9	-0.445091, -0.609329, -0.103336
15	15268.4	-0.659273, -0.880466, -0.218877
16	-82948.9	0.272727, -0.653061, -0.853539
17	-88888.9	-0.527273, -0.201166, -1
18	88888.9	-0.527273, -0.58309, -0.685924
19	-88888.9	0.272727, -0.0612245, -1
20	88888.9	-0.527273, -0.921283, -0.661513
21	88888.9	-0.527273, -0.994169, 0.0903173
22	-20775.4	-0.62, -0.058309, 1
23	-88888.9	-0.445091, -0.623907, -0.0707893
24	-88888.9	-0.781818, -0.892128, -0.602929
25	88888.9	-0.927273, -0.708455, -0.567128
26	-88888.9	-0.781818, -0.825073, -0.793328
27	-88888.9	-1, -0.723032, -0.609439
28	-88888.9	-0.781818, -0.725948, -0.79821
29	64448.1	-0.563636, -0.102041, -0.18633
30	88888.9	-0.527273, -0.83965, -0.552482
31	-88888.9	-0.781818, -0.825073, -0.593165
32	-88888.9	-0.625455, -0.609329, -0.389748
33	88888.9	-0.195273, -0.883382, -0.562246
34	-56839.3	-0.236364, -0.548105, -0.910496
35	88888.9	-0.610909, -0.650146, -0.585028
36	-88888.9	-0.527273, -0.994169, 0.0903173
37	88888.9	-0.527273, -0.714286, -0.768918
38	88888.9	-0.527273, -0.810496, -0.66965
39	-88888.9	-0.549091, -0.376093, -0.607811
40	-88888.9	1, 0.48105, -0.728234
41	88888.9	-1, -0.183673, -1
42	-88888.9	-0.563636, -0.568513, -0.121237
43	88888.9	-0.2, -0.440233, -0.973963
44	-88888.9	-0.236364, -0.696793, -0.495525
45	-88888.9	-0.549091, -0.795918, -0.607811
46	-88888.9	-0.745455, -0.883382, -0.685924
47	-88888.9	-0.625455, -0.915452, -0.389748
48	-88888.9	-0.549091, -0.795918, -0.607811
49	15537.1	-0.236364, -0.358601, -0.104963
50	-88888.9	-0.781818, -0.810496, -0.710334
51	-88888.9	-0.927273, -0.708455, -0.542718
52	-88888.9	-1, -0.728863, -0.853539
53	-88888.9	-0.549091, -0.376093, -0.607811
54	-88888.9	-0.527273, -0.632653, -0.853539
55	-88888.9	-0.625455, -0.609329, -0.389748
56	88888.9	1, 0.300292, -0.728234
57	88888.9	-0.8, -0.763848, -0.542718
58	-88888.9	-0.527273, -0.623907, -0.853539
59	-88888.9	-0.549091, -0.376093, -0.607811
60	88888.9	-0.236364, -0.358601, -0.462978
61	-88888.9	-0.236364, -0.381924, -0.332791
62	-88888.9	-0.563636, -0.516035, -0.21725
63	-88888.9	-0.0527273, -0.883382, -0.62083
64	-88888.9	1, 0.48105, -0.728234
65	88888.9	1, -0.0174927, -0.728234
66	88888.9	-0.236364, -0.381924, -0.576892
67	-88888.9	-0.781818, -0.714286, -0.710334
68	-88888.9	-0.549091, -0.795918, -0.607811
69	-88888.9	-0.527273, -0.705539, -0.775427
70	-68863.3	-0.818182, -0.854227, -0.809601
71	88888.9	-0.610909, -0.921283, -0.529699
72	-88888.9	-0.781818, -0.825073, -0.793328
73	88888.9	-0.8, -0.755102, -0.554109

74	-88888.9	-0.8, -0.460641, -0.570382
75	11261.1	0.0909091, -0.638484, -0.907242
76	88888.9	-0.527273, -0.723032, -0.545972
77	-88888.9	-0.808727, -0.629738, -0.601302
78	-67882.2	1, 0.300292, -0.728234
79	88888.9	-0.745455, -0.892128, -0.674532
80	-45345.3	-0.62, -0.428571, 1
81	-42824	-0.236364, 0.0408163, -0.495525
82	-88888.9	-0.625455, -0.915452, -0.389748
83	88888.9	-0.818182, -0.708455, -0.542718
84	-88888.9	-0.345455, -0.793003, -0.915378
85	-88888.9	-0.694909, 0.638484, 0.404394
86	88888.9	-0.625455, -0.03207, -0.389748
87	-88888.9	-0.745455, -0.801749, -0.668023
88	88888.9	-0.659273, -0.912536, -0.228641
89	-88888.9	-1, -0.35277, -0.853539
90	-88888.9	-0.195273, -0.947522, -0.663141
91	-88888.9	-0.781818, -0.720117, -0.705452
92	88888.9	-0.527273, -0.548105, -0.664768
93	88888.9	-0.818182, -0.690962, -0.809601
94	84913.5	1, 0.48105, -0.728234
95	-64583.4	0.272727, -0.35277, -0.853539
96	88888.9	-0.302545, -1, 0.977217
97	-88888.9	-0.625455, -0.915452, -0.389748
98	88888.9	-0.745455, -0.723032, -0.785191
99	26851.2	-0.62, 0.317784, -0.158666
100	88888.9	-0.625455, -0.411079, -0.389748
101	-45264.7	-0.527273, -0.373178, -0.853539
102	37881.6	-0.62, -0.0408163, -0.158666
103	-88888.9	-0.709091, -0.892128, -0.783564
104	-88888.9	-0.781818, -0.822157, -0.697315
105	88888.9	-1, -0.620991, -0.853539
106	17141.9	0.0545455, -0.889213, -0.729862
107	-88888.9	-1, -0.635569, -0.609439
108	88888.9	-0.563636, -0.580175, -0.103336
109	-88888.9	-0.527273, -0.623907, -0.853539
110	88888.9	-0.781818, -0.941691, -0.62083
111	70264.4	-1, -0.35277, -0.853539
112	74879.8	-0.527273, -0.201166, -1
113	88888.9	-0.563636, -0.332362, -0.13751
114	88888.9	-0.418182, -0.830904, -0.913751
115	-88888.9	-0.418182, -0.833819, -0.910496
116	88888.9	-0.527273, -0.927114, -0.653377
117	88888.9	-0.563636, -0.883382, -0.178194
118	-88888.9	-0.62, -0.539359, 1
119	88888.9	-0.527273, -0.539359, -0.882832
120	88888.9	-0.527273, -0.74344, -0.889341
121	-41855.7	-0.445091, -0.61516, -0.0919447
122	88888.9	-0.563636, -0.883382, -0.178194
123	88888.9	-0.818182, -0.690962, -0.809601
124	81511.7	0.272727, -0.0466472, -1
125	88888.9	-0.527273, -0.620991, -0.762408
126	-88888.9	-0.745455, -0.723032, -0.830757
127	-87959.5	-0.302545, -0.997085, 0.973963
128	-63222	-0.345455, -0.787172, -0.918633
129	-88888.9	-0.659273, -0.906706, -0.493897
130	-88888.9	-0.709091, -0.877551, -0.801465
131	88888.9	-0.709091, -0.758017, -0.791701
132	88888.9	0.272727, -0.626822, -0.853539
133	88888.9	-0.527273, -0.708455, -0.542718
134	88888.9	-0.659273, -0.944606, -0.627339
135	88888.9	-0.8, -0.83965, -0.536208
136	-88888.9	-0.625455, -0.915452, -0.389748
137	-88888.9	-0.527273, -0.816327, -0.664768
138	57766.8	-0.62, -0.539359, 1
139	-88888.9	-0.625455, -0.810496, -0.389748
140	88888.9	-0.527273, -0.696793, -0.558991
141	88888.9	-0.527273, -0.755102, -0.882832
142	88888.9	-0.8, -0.641399, -0.578519
143	88888.9	-0.527273, -0.816327, -0.560618
144	88888.9	-0.563636, -0.819242, -0.13751
145	-88888.9	0.272727, -0.725948, -0.609439
146	-88888.9	-0.236364, -0.588921, -0.726607
147	88888.9	-0.527273, -0.819242, -0.555736
148	88888.9	-0.745455, -0.723032, -0.830757
149	88888.9	-0.898182, -0.883382, -0.627339
150	88888.9	-0.527273, -0.54519, -0.66965
151	-88888.9	-0.236364, -0.594752, -0.495525

152	88888.9	-0.709091, -0.900875, -0.7738
153	88888.9	-0.818182, -0.854227, -0.809601
154	88888.9	0.272727, -0.367347, -0.853539
155	-88888.9	-1, -0.720117, -0.609439
156	88888.9	-0.8, -0.501458, -0.539463
157	-88888.9	-0.709091, -0.588921, -0.788446
158	88888.9	-0.610909, -0.705539, -0.521562
159	88888.9	-1, -0.632653, -0.853539
160	88888.9	-0.898182, -0.612245, -0.656631
161	88888.9	-0.0527273, -0.915452, -0.557364
162	88888.9	-0.745455, -0.77551, -0.558991
163	-27416.4	-1, -1, -1
164	-88888.9	-0.625455, 1, -0.389748
165	-5921.62	-1, -0.0466472, -1
166	88888.9	-0.62, 0.294461, 1
167	-88888.9	-0.781818, -0.895044, -0.599675
168	88888.9	-0.236364, -0.597668, -0.889341
169	-88888.9	-0.781818, -0.83965, -0.570382
170	84743.2	-0.694909, 0.638484, 0.404394
171	88888.9	-0.709091, -0.758017, -0.791701
172	88888.9	-0.610909, -0.0932945, -0.570382
173	-88888.9	-0.625455, -0.609329, -0.389748
174	-88888.9	-0.563636, -0.0670554, -0.215622
175	-14218	0.272727, -0.728863, -0.609439
176	-88888.9	-0.709091, -0.594752, -0.783564
177	-80821.4	-0.62, 0.294461, 1
178	-88888.9	-0.549091, -0.795918, -0.607811
179	-88888.9	-0.527273, -0.591837, -0.677787
180	62825.9	-0.625455, -0.03207, -0.389748
181	-88888.9	-0.625455, -0.810496, -0.389748
182	-88888.9	-0.781818, -0.825073, -0.593165
183	88888.9	-0.890909, -0.708455, -0.567128
184	-19957.2	-0.527273, -0.994169, 0.0903173
185	-88888.9	-0.527273, -0.845481, -0.542718
186	-51260.4	-1, -0.626822, -0.609439
187	-88888.9	-0.709091, -0.77551, -0.778682
188	-88888.9	-0.625455, -0.810496, -0.389748
189	88888.9	-0.236364, -0.358601, -0.283971
190	-122.445	1, 1, 1
191	88888.9	-0.527273, -0.539359, -0.672905
192	88888.9	-0.898182, -0.6793, -0.593165
193	88888.9	-0.527273, -0.553936, -0.874695
194	-88888.9	-0.781818, -0.813411, -0.708706
195	-88888.9	-0.709091, -0.580175, -0.791701
196	88888.9	0.272727, -0.731778, -0.609439
197	88888.9	-0.185455, -0.723032, -0.965826
198	88888.9	-0.610909, -0.845481, -0.554109
199	88888.9	0.0545455, -0.854227, -0.7738
200	-88888.9	-0.563636, -0.311953, -0.163548
201	88888.9	-0.818182, -0.941691, -0.809601
202	18318.5	-0.527273, -0.48105, 0.0903173
203	-88888.9	1, 0.48105, -0.728234
204	88888.9	1, 0.48105, -0.728234
205	88888.9	-0.781818, -0.740525, -0.684296
206	88888.9	-0.898182, -0.842566, -0.640358
207	58986.2	-0.236364, -0.594752, -0.495525
208	88888.9	-0.745455, -0.772595, -0.702197
209	88888.9	-0.563636, -0.895044, -0.13751
210	-88888.9	-0.62, 0.950437, 1
211	88888.9	-0.563636, -0.294461, -0.178194
212	-88888.9	-0.62, -0.527697, -0.158666
213	-88888.9	-0.625455, -0.03207, -0.389748
214	-68085.4	1, -0.0174927, -0.728234
215	88888.9	-0.236364, -0.212828, -0.495525
216	86645.2	-0.781818, -0.717201, -0.804719
217	88888.9	1, 0.48105, -0.728234
218	-88888.9	-0.745455, -0.778426, -0.697315
219	88888.9	-0.527273, -0.798834, -0.583401
220	-88888.9	-0.563636, -0.12828, -0.163548
221	-5234.68	-0.709091, -0.769679, -0.783564
222	88888.9	-0.709091, -0.886297, -0.790073
223	-23562.1	-0.236364, -0.594752, -0.332791
224	88888.9	-0.527273, -0.921283, -0.661513
225	-88888.9	-0.195273, -0.932945, -0.539463
226	-88888.9	-0.625455, 1, -0.389748
227	88888.9	-0.781818, -0.938776, -0.624085

228	88888.9	-0.527273, -0.723032, -0.545972
229	-88888.9	-0.527273, -0.941691, -0.755899
230	88888.9	1, 0.48105, -0.728234
231	88888.9	-0.610909, -0.862974, -0.521562
232	-88888.9	-0.659273, -0.906706, -0.646867
233	-88888.9	-0.625455, -0.03207, -0.389748
234	88888.9	-0.62, -0.428571, 1
235	-88888.9	-0.8, -0.827988, -0.557364
236	88888.9	-0.818182, -0.941691, -0.809601
237	72388.5	-0.927273, -0.708455, -0.542718
238	-88888.9	-0.781818, -0.895044, -0.599675
239	-88888.9	-0.527273, -0.629738, -0.755899
240	88888.9	-0.781818, -0.708455, -0.567128
241	88888.9	-0.527273, -0.379009, -0.853539
242	-88888.9	-0.236364, -0.565598, -0.903987
243	-88888.9	-0.625455, -0.03207, -0.389748
244	88888.9	-0.62, 0.982507, -0.158666
245	88888.9	1, -0.227405, -0.728234
246	88888.9	-0.195273, -0.892128, -0.612693
247	-88888.9	-0.781818, -0.819242, -0.799837
248	-88888.9	-0.527273, -0.734694, -0.752644
249	10221.4	-1, -0.728863, -0.853539
250	-88888.9	0.0909091, -0.629738, -0.910496
251	88888.9	-0.527273, -0.825073, -0.653377
252	-88888.9	-0.527273, -0.93586, -0.76729
253	-57612.8	-0.527273, -0.842566, 0.0903173
254	88888.9	-0.625455, 1, -0.389748
255	-88888.9	-0.236364, -0.381924, -0.495525
256	88888.9	-0.610909, -0.137026, -0.545972
257	-80999.7	-0.709091, -0.594752, -0.783564
258	-70972.9	-0.195273, -0.96793, -0.668023
259	-88888.9	-0.781818, -0.71137, -0.809601
260	-88888.9	-0.334545, -0.457726, -0.908869
261	-87673.6	-0.62, 0.982507, -0.158666
262	-1584.33	-0.625455, 1, -0.389748
263	-66672.8	-0.236364, -0.381924, -0.495525
264	88888.9	-0.625455, 1, -0.389748
265	-88888.9	-0.625455, -0.915452, -0.389748
266	-88888.9	1, -0.0174927, -0.728234
267	88888.9	1, 0.48105, -0.728234
268	88888.9	-0.527273, -0.749271, -0.887714
269	88888.9	-0.898182, -0.819242, -0.617575
270	-38777	1, -0.399417, -0.728234
271	-88888.9	1, 0.48105, -0.728234
272	88888.9	-0.527273, -0.737609, -0.894223
273	88888.9	-0.527273, -0.717201, -0.532954

Controlling A Robotic Arm Using Handwritten Digit Recognition Software

Ali Cetinkaya*‡, Onur Ozturk**, Ali Okatan***

* Technology Transfer Office, Istanbul Gelisim University, Avcılar, Istanbul, Turkey.

** School of Management, Faculty of Engineering, University College London (UCL), Euston, London, UK.

*** Department of Computer Engineering, Faculty of Engineering, Istanbul Gelisim University, Avcılar, Istanbul, Turkey.

(alcetinkaya@gelisim.edu.tr, onur.ozturk.16@ucl.ac.uk, aokatan@gelisim.edu.tr)

‡ Corresponding Author: Ali Cetinkaya, Technology Transfer Office, Istanbul Gelisim University, Avcılar, Istanbul, Turkey. Tel: +90 212 422 70 00 / 7187. alcetinkaya@gelisim.edu.tr

Received: 21.09.2018 Accepted:30.1.2019

Abstract- Repetitive tasks in the manufacturing industry is becoming more and more commonplace. The ability to write down a number set and operate the robot using that number set could increase the productivity in the manufacturing industry. For this purpose, our team came up with a robotic application which uses MNIST data set provided by Tensor flow to employ deep learning to identify handwritten digits.

The system is equipped with a robotic arm, where an electromagnet is placed on top of the robotic arm. The movement of the robotic arm is triggered via the recognition of handwritten digits using the MNIST data set. The real time image is captured via an external webcam. This robot was designed as a prototype to reduce repetitive tasks conducted by humans.

Keywords MNIST Handwritten Digit Recognition, Deep Learning, Embedded System Robotic Arm Control

1. Introduction

The MNIST dataset was created using two datasets from the US National Institute of Standards and Technology (NIST). Training data set includes handwritten digits from approximately 250 people, where half of these people are high school students and the other half is the employees of the Census Bureau. The data set consists of 60,000 training digits and 10,000 test digits. Having such a huge number of data allows the software to identify handwritten digits of many types of handwriting. Furthermore, this allows our system to be used by many people due to the inclusiveness of the training and test data sets [1].

Keras is a high-level neural networks API, written in Python and capable of running on top of TensorFlow, CNTK, or Theano [2]. Keras was developed with ease of experimentation and speed in mind, therefore it is highly favoured by researchers. In our system, we used Keras API to create a 7-layer Convolution Neural Network (CNN) [3][4]. The layers were convolution, pooling, convolution, convolution, pooling, activation and identification respectively. The compilation of 15 epochs, which gives out 99.4% accuracy, takes around 40 minutes per epoch on a CPU-only computer.

Today, developments in robotics are concentrated in a number of areas. These areas are mainly about the imaging systems of robots, artificial intelligence and machine learning. In robotic imaging systems, it is the process of capturing and defining the images of objects and finding the coordinates of the specified objects. This is the process of performing the action of the robot according to coordinates after the defined movement [10, 12]. In terms of human health, there are situations where it is not possible to work in dangerous environments. For this purpose, the robot arm was operated by the sensors placed on the human arm [11]. In the studies developed on image processing, image classification and image extraction are the most important processes. At this point, that accuracy affects the success of the study [13]. The images taken from the camera define the color and shape of the object. The system applies the center-based calculation, filtering and color segmentation algorithm to locate the target and the position of the robot arm [14].

The image recognition software was designed in OpenCV3, whereas the embedded system was designed in Arduino. The hardware system is shown in Fig. 1.

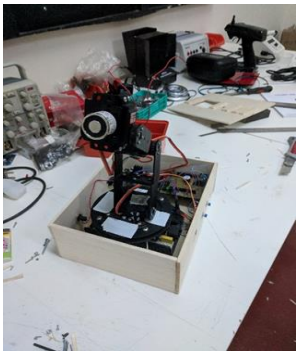

Fig. 1. Hardware layout of the system

Robot Kinematics is a geometrical study of the structure of a robot and independent of dynamic effects such as force and torque. The results of these kinematic investigations are obtained from the robots regarding the position, speed and acceleration of the joints and the final limb. The analysis of the robot requires knowledge of many branches of science, such as Mathematics, Mechanics and electronics [15, 16].

The robotic system is capable of operating for pre-defined actions in Arduino. There are four actions defined in Arduino being: moving the arm forwards, turning on the electromagnet, moving the arm backwards and turning off the electromagnet. The numbers to be identified to get into action for each operation is 2, 3, 4 and 5 respectively.

2. Hardware

Power source 12V is the required voltage for the system to work. The city grid provides the robot with 220V of electricity, therefore the power source is responsible for converting the 220V to 12V for the robot to work.

Servo engines present in the system to accurately control the robotic arm. These servo engines are capable of moving between 0 – 180 degrees however, during this experiment, the angles never exceeded 30 and 150 respectively, in order not to damage the servos. Furthermore, having three servos present in the robot alleviates the need for using the servo engines at their maximum capacity; using three servos in parallel gives the arm extended movement space.

The servo engine controller receives the movement signals from the Arduino Mega present in the system. Furthermore, servo engine controller receives 5V from regulator in order to move the servos. Both the signals from Arduino Mega and regulator are then used to control the robotic arm.

The purpose of the relay in the system to control the status of the electromagnet. This is supported by the signals received from Arduino Mega according to user input. The embedded timer in Arduino Mega excels as compared to many other Arduino boards. The system runs with three servo engines therefore the timing between the servo engines to move them to the desired angles was important and the library of Arduino Mega was the most adequate for this operation.

As previously mentioned, the system receives 12V of energy, however servos require 5V of energy to work. The regulator is responsible for converting 12V coming into the system to 5V to feed them into the servos for operation.

The electromagnet works with 12V of energy. Given the size of this prototype robot, an electromagnet with a maximum pulling force of 50N (5 kilograms) was used in order to avoid the robot from tipping over. The electromagnet can be seen in Fig. 2. along with the closed system.

Fig. 2. Fully working, closed system.

3. Embedded System and Software Algorithm's

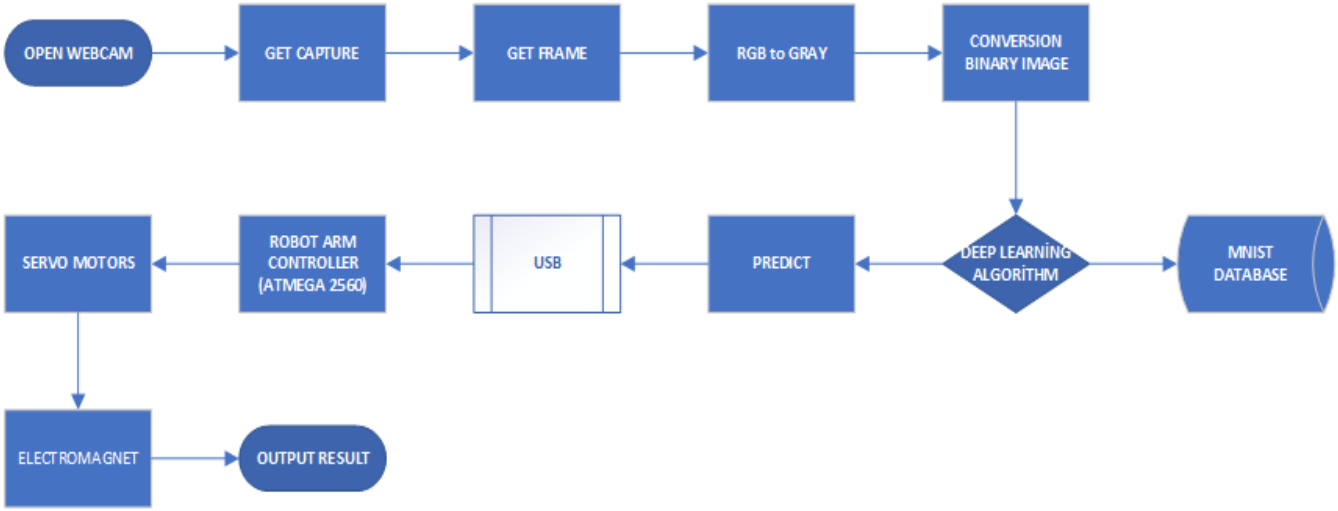

Fig. 3 Flow diagram of algorithm step.

Defining mathematical figures is an important problem. In this study using the deep learning algorithm and MNIST data set consists of 5 main stages. These are: pre-processing on the image, feature extraction, deep learning algorithm, MNIST data set and microcontroller control. The handwritten robotic arm control architecture is shown in Fig. 3.

3.1. Embedded System Control

The embedded system was developed with atmel atmega2560 microcontroller using embedded c for programming. The embedded system was designed Arduino Mega code was produced in the Arduino IDE. The Arduino software is responsible for operating the robot. This is done via data received from the MNIST Handwritten Digit Recognition Software, which is written in Python. Arduino was chosen language due to the availability robotic libraries for ease of control [5].

In the first segment of the Arduino code, the variables were declared. In this segment, there are pin declarations, servo declarations and servo angle declarations.

In the setup () segment of the code, the servos were connected to their respective pins. Furthermore, the initiation angles of the three servos were declared. The initiation angles are 90 degrees for each servo. These values help the user understand that the system has initiated because there is no user input that can keep the servos at 90 degrees. After setting the servos to their angles, the serial port connection was opened. The user can understand the connection has been established via the three-note music played by the buzzer present in the system. This serial connection allows the Arduino code to interact with the signals received from the Python code.

Finally, in the loop () section of the code, a switch case was created. The Python code sends off letters ranging from ‘a’ to ‘e’, and each letter is assigned to an action in the robot. The switch case is responsible for controlling which action is triggered according to the input received from Arduino.

3.2. MNIST Handwritten Digit Recognition Software

The Python digit recognition software works using OpenCV and Serial Port [6]. OpenCV proves rather useful when working with computer vision and image recognition due to wide variety of supported libraries and conducted experiments. “OpenCV has more than 47 thousand people user community and estimated number of downloads exceeding 14 million. Usage ranges from interactive art, to mines inspection, stitching maps on the web or through advanced robotics.” [6].

When the software is initiated, a video stream from the camera of the PC (or webcam, in this system) is recorded and presented on the screen. Even though the entire video stream is presented on the screen, the part of the screen which processes the information is marked with a blue square. Instead of detecting the entire video stream, the blue square was chosen to be area of interest due to efficiency purposes. The program works more efficiently in a smaller area. The user must present his/her handwritten in this square for the software to process the information. Once the handwritten is presented in this square, the software is responsible for counting the empty spaces between the handwritten digits. For example, if the software is counting 3 defects, there would be 4 handwritten present in the square, which would trigger an action to the servos.

The MNIST database consists of 70,000 samples of handwritten digits. Each of them is grayscale image of size 28px x 28px. The software initiates by capturing the presented handwritten digit from the external camera. Furthermore, a label on the top right of this extracted digit is placed to indicate which number is predicted for this extracted image. Then, the extracted image is translated into grayscale. The purpose of having a greyscale image is because OpenCV has built in libraries that work with grayscale image [6].

The process is to predict the handwritten digit in this grayscale image. This grayscale image is then fed into the CNN. The first layer type of layer, which is convolution, is responsible for filtering out the images to increase processing speed. The second type of layer is pooling, which is present to reduce the risks of overfitting. This type of layer reduces the parameters to be learnt and in return reduces noise within the image. The third type of layer is activation, which is where the CNN learns the properties of the images. Our system works with ReLU activation function, which is chosen for its benefits when it comes to representing a large range of numeric values. The final layer is the fully-connected layer, which represents the functionality of an Artificial Neural Network. Each node in the previous layer is connected to each other node in the upcoming layer. This process helps the CNN compare features from the inputted image with the training data set to predict the outcome of the handwritten digit [7-9].

The Python code can be seen alongside the closed system can be seen in Fig. 4.

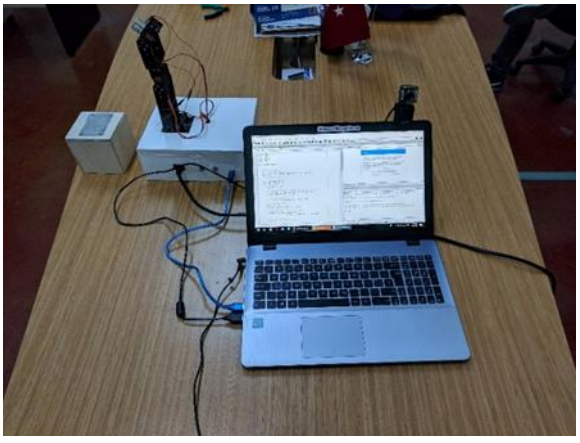

Fig. 4. Closed system along with the software.

4. Kinematic Analysis

Kinematic analysis generates kinematic equations describing robot motion geometry. Using the mechanical properties of the robot, forward kinematic analysis is required

in order to hold an object with electromagnet and leave it to a desired target. In doing these movements, inverse kinematic analysis is required to find the angles to which the joints should be found.

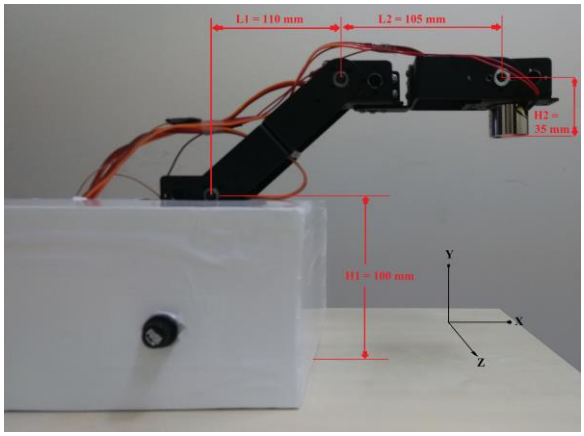

Fig. 5. Length and axis information of the robot arm.

Fig. 5. shows the part lengths and axis information of the robot arm.

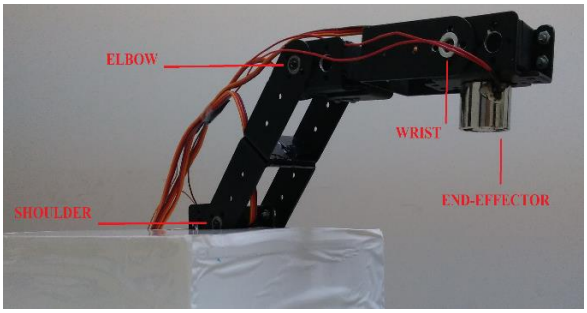

Fig. 6. Length and joint definitions of robot arm limbs

Fig. 6. shows the length of the shoulder, base, shoulder, elbow and wrist joints are formed. In addition, the robot arm has a holder end used to grasp objects.

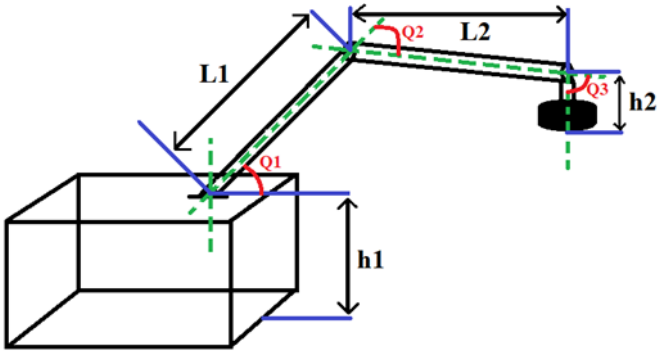

Fig. 7. Design details of robot arm parts.

As shown on Fig. 7. the robot arm lengths are L1 and L2. Height h1 between robot base and L1 arm, the height between the holder electromagnatis and the wrist on the L2 handle is known to be H2. Forward kinematic analysis of the robot through this data;

$$x = L_1*\cos\theta_1+L_2*\cos(\theta_1+\theta_2)+L_3*\cos(\theta_1+\theta_2+\theta_3) \quad (1)$$

$$y = L_1*\sin\theta_1+L_2*\sin(\theta_1+\theta_2)+L_3*\sin(\theta_1+\theta_2+\theta_3) \quad (2)$$

$$\theta = \theta_1+\theta_2+\theta_3 \quad (3)$$

We'II find out where the electromagnet on the robot arm is in the work area. If the robot arm is taken derivative of the above equations according to time to find the speed of operation,

$$x' = -L_1*\theta_1'*\sin\theta_1-L_2*(\theta_1'+\theta_2')*\sin(\theta_1+\theta_2)-L_3*\cos(\theta_1'+\theta_2'+\theta_3')*\sin(\theta_1+\theta_2+\theta_3) \quad (4)$$

$$y' = L_1*\theta_1'*\cos\theta_1+L_2*(\theta_1'+\theta_2')*\cos(\theta_1+\theta_2)+L_3*\cos(\theta_1'+\theta_2'+\theta_3')*\cos(\theta_1+\theta_2+\theta_3) \quad (5)$$

$$\theta' = \theta_1'+\theta_2'+\theta_3' \quad (6)$$

According to the data above, speed equations (4), (5) and (6) are found.

The Robot calculates the angle θ1 and θ2 where the joints should be located with Inverse Kinematics while making their movements with forward kinematics. These angle equations are given in equation (7) and (8).

$$\theta_1 = tan^{-1}\frac{y}{x} + tan^{-1}\frac{L_2*\sin\theta_2}{L_1+L_2*\cos\theta_2} \quad (7)$$

$$\theta_2 = -cos^{-1}\frac{x^2+y^2-L_1^2-L_2^2}{2*L_1*L_2} \quad (8)$$

Given above (1), (2), (3), (7) and (8) equations of the robot arm X, Y coordinates and θ angles are calculated. The angles θ1 and θ2 of the servo motors on the robot arm are calculated.

Fig. 8. shows four working positions of the robot arm. These locations show the points needed to perform the robot's tasks.

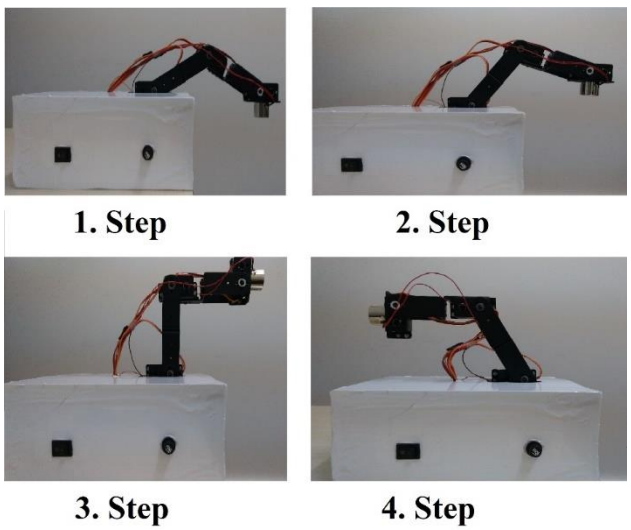

Fig. 8. 4 different motion results of the robot arm view.

5. Experiments

In the test environment, a snapshot of the numbers on the white background is taken and the operations are performed. Tests have been repeated by changing the distance between the texts and the display device. The test environment is given in Fig. 9.

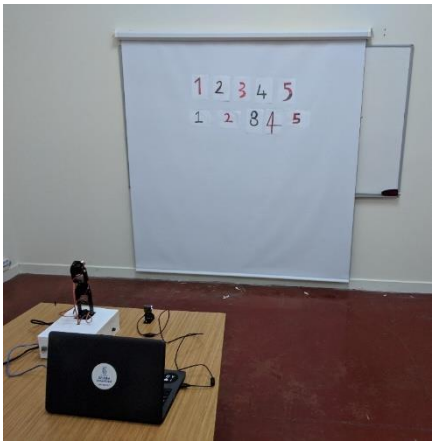

Fig. 9. Showcase of the system

In this experiment, the distance between the background and the camera was 30 centimeters. The purpose of this experiment was to test whether the software is capable of recognizing digits from a relatively short distance. The handwriting figures used in the experiment are written by the authors of this article and shown on Fig. 10. The handwritten digits for Onur Ozturk and Ali Cetinkaya respectively are presented below.

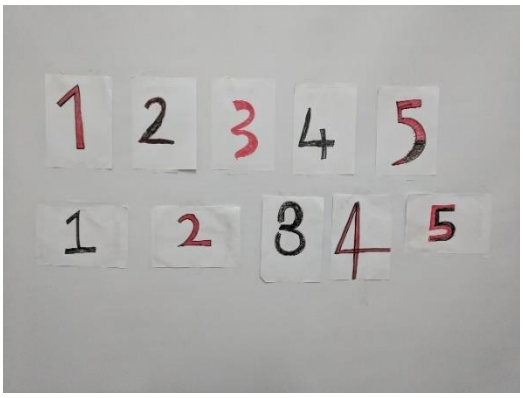

Fig. 10. Testing data set

Recognizing digits from a distance of 30cm between the background and camera.

The handwritten digits presented above were tested individually and the results received from these tests are presented below. Some figures resulted in incorrect predictions, however the majority of the predictions are correct.

The screenshots of the experiments performed between Figure 11 and Figure 26 are given.

Fig. 11. Incorrectly predicted ‘1’.

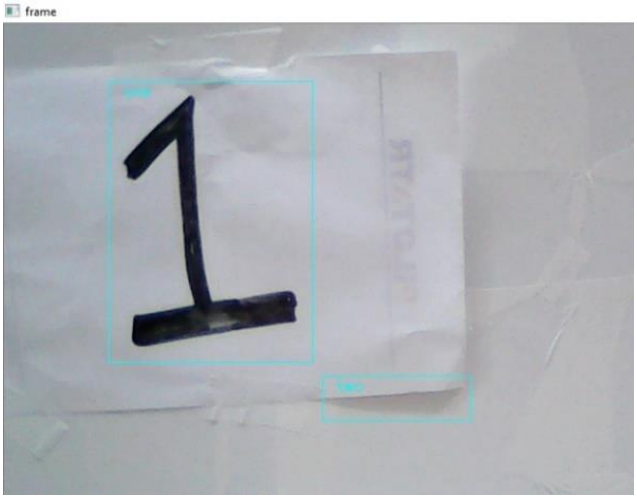

Fig. 12. Correctly predicted ‘1’.

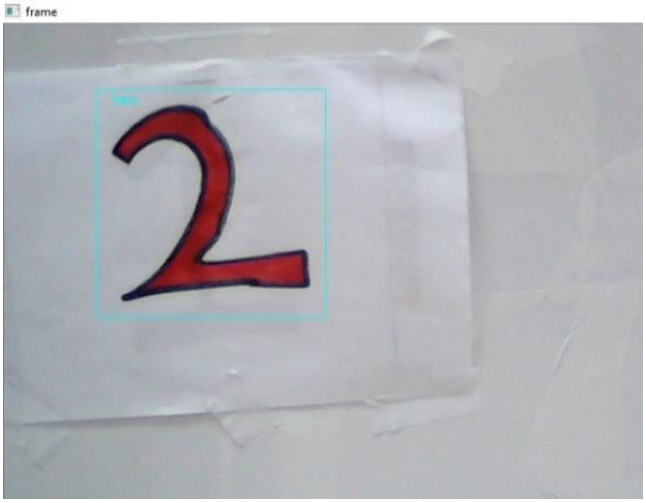

Fig. 13. Correctly predicted ‘2’.

Fig. 14. Correctly predicted '3'.

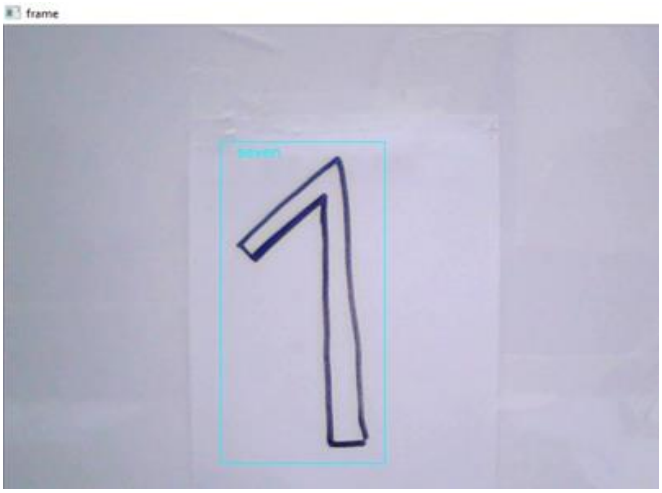

Fig. 17. Incorrectly predicted '1'.

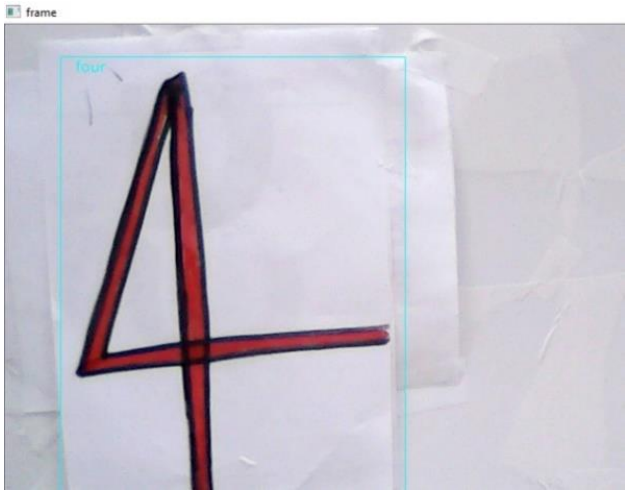

Fig. 15. Correctly predicted '4'.

Fig. 18. Correctly predicted '2'.

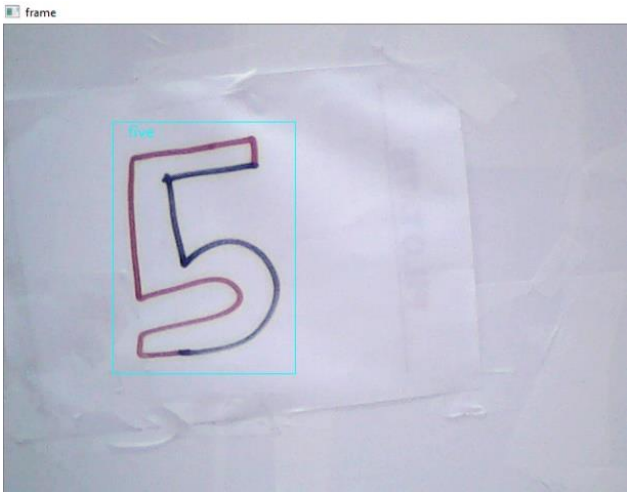

Fig. 16. Correctly predicted '5'.

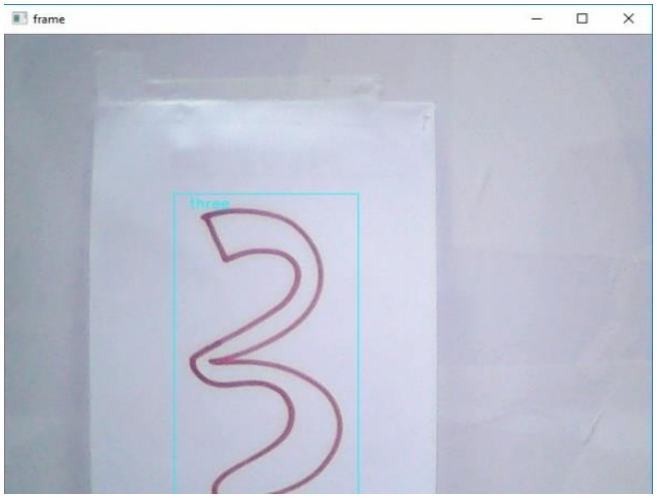

Fig. 19. Correctly predicted '3'.

Fig. 20. Incorrectly predicted ‘4’.

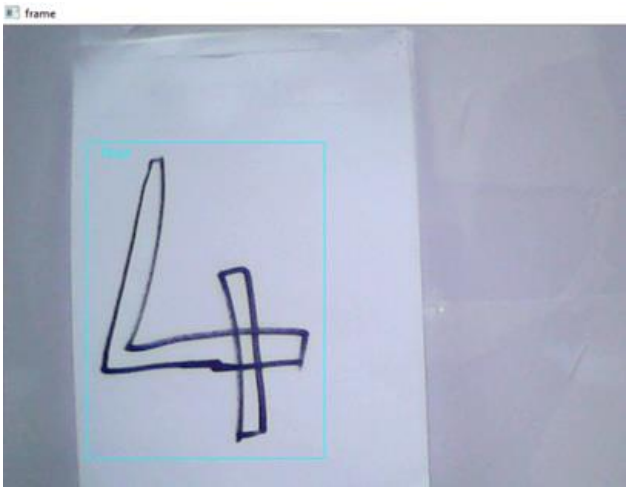

Fig. 21. Correctly predicted ‘4’.

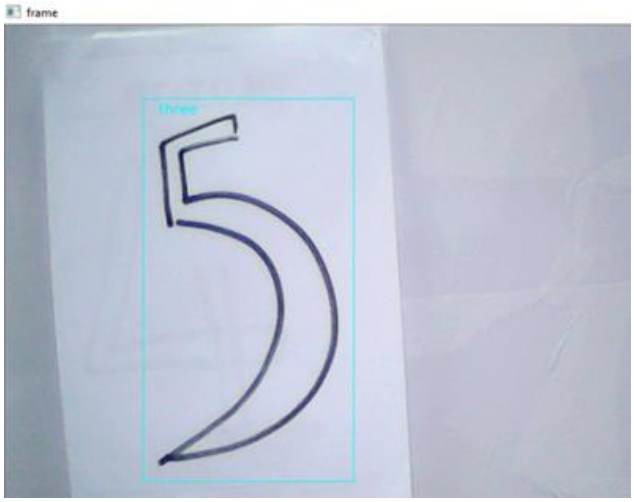

Fig. 22. Incorrectly predicted ‘5’.

In this experiment, the distance between the background and the camera was 2 meters. The purpose of this experiment was to test whether the software is capable of recognizing digits from a long distance. The test data set was presented in the previous section.

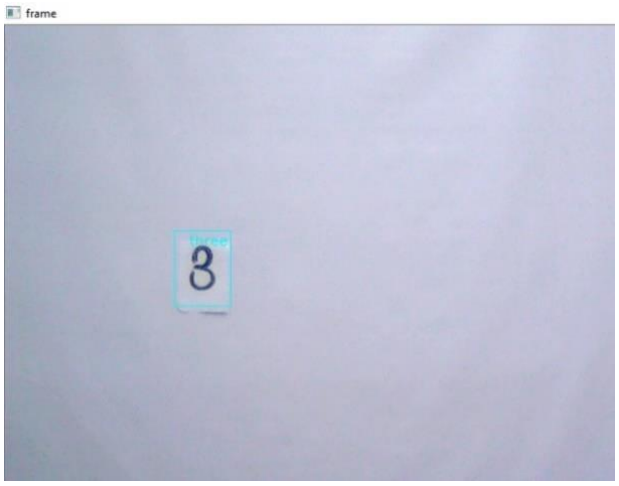

Fig. 23. Correctly predicted ‘3’.

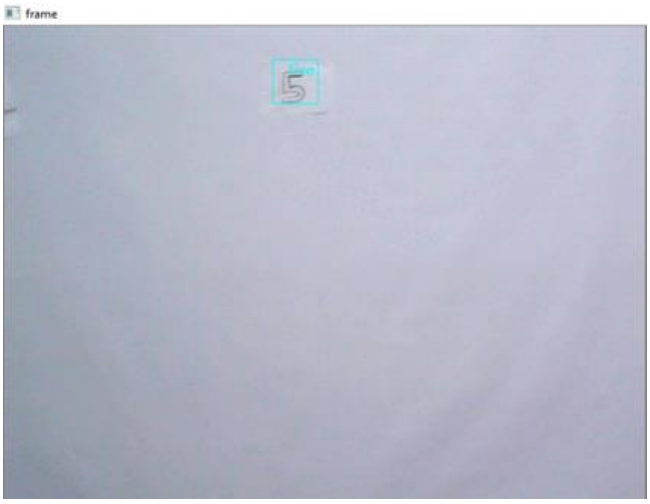

Fig. 24. Correctly predicted ‘5’.

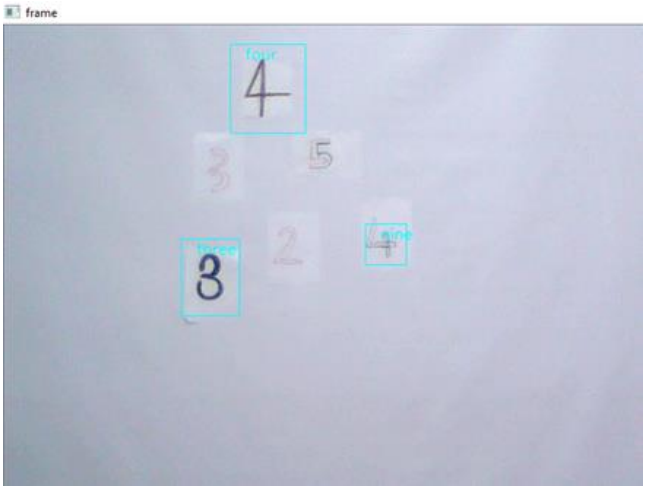

Fig. 24. Showcasing the importance of boldness from a distance of 2m.

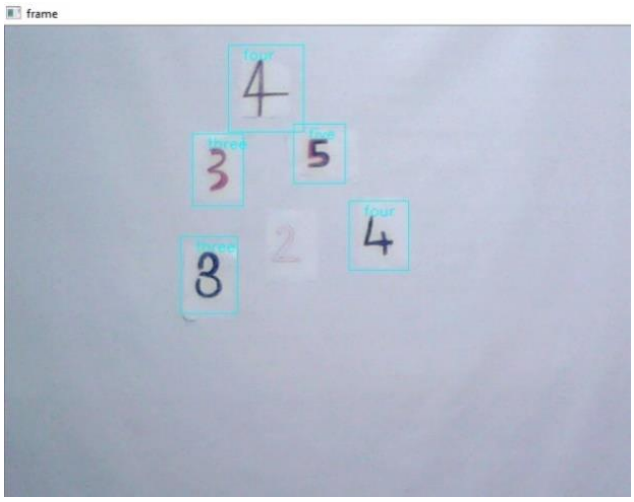

Fig. 25. Further showcasing the importance of boldness from a distance of 2m.

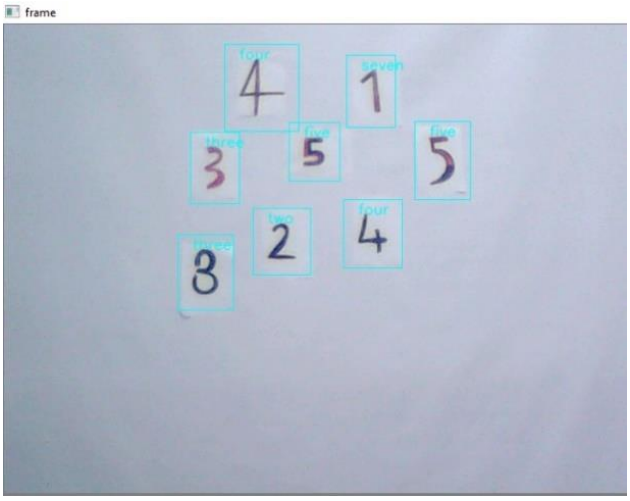

Fig. 26. Results achieved from a mixed test set.

The first issue arises from the distance at which the software is capable of recognizing the handwritten digits. From a short distance, writing the numbers with a black or red board marker was sufficient. However, as the distance between the board on which the digits were written and the camera increases, the software had difficulty recognizing the numbers. The nature of the problem is caused by the thickness of the digits written. From a short distance, the thickness of the board marker was sufficient however from a long distance, it looked thin therefore the camera could not recognize the digits.

The second issue arises from having an unstable board and camera. When conducting the tests for the system, the team realized that if either the camera or the board was shaking, the software could not identify the digits. To solve this issue, we fixed the camera to a book and the handwritten digits were stuck to the board with tape. Furthermore, if the paper with the digit written on it is not stuck to the background completely where some part of the paper is lifting off, the shadows left by the lifting paper is recognized by the software as handwritten digits. Therefore, the paper with the digit must be completely stuck to the background where no piece is lifting off the background.

The third issue arises from not having the handwritten digit completely within the frame. For example, during the testing phase when number four were shown to the camera whilst not being within the frame fully, the software recognized this number as six. In order to achieve correct recognition, the most optimal position for the handwritten digit is the middle of the frame. This issue is presented in the Experiment and Results section in Figures 9 and 10.

The final issue arises from the similarity of the digit ‘1’ and ‘7’. During our tests, different members of the team wrote different ‘1’s, where the horizontal line on the bottom was not present in some handwritten digits. The MNIST data set trained ‘1’s with the horizontal line present. Therefore, when a person did not include the horizontal line below ‘1’, the software recognized the digit as ‘7’. This issue is presented in the Experiment and Results section in Figures 9.7.

6. Conclusion

The results indicated that as the distance between the background and the camera increases, the boldness of the handwritten digits must increase in order for the camera to capture the image presented on the background. Furthermore, a special case for number ‘1’ and ‘7’ exists. The user must include the horizontal line below the ‘1’ in order for the software to predict the number correctly as ‘1’. This is most likely caused by the training data set including the horizontal line below ‘1’s.

In the results obtained, it was observed that the robot performs the movements given in Figure 8 according to the order of identification. Because there are no lines below 1 characters created for testing, MNIST could not find them in the data set and incorrectly confused them with 7 characters.

7. Discussion

In this study, a system has been developed with an electromagnet placed on a robotic arm to perform repetitive processes in the manufacturing industry. For this purpose, the numbers of "1, 2, 3, 4, 5" written by hand on the MNIST dataset were detected and recognized through the camera.

During the experiments, 17 samples were taken from the images taken from the camera. In these experiments, 12 samples had correct results, 5 samples had false results and 2 samples had incomplete readings.

One of wrong reading "1" when there is no horizontal line under a character "7" has been observed to interfere with the character.

The figures used in the study were created by Onur OZTURK and Ali CETINKAYA. As the distance between the background and the camera increases in the experiments, it is concluded that the numbers need to be thickened so that the software can capture the image. To correct this error, the reading resolution and accuracy can be increased by increasing the camera resolution.

Acknowledgements

Many thanks to Istanbul Gelisim University and Technology Transfer Office for their support.

References

[1] Y. Lecun, C. Cortes, C.J.C. Burges, MNIST handwritten digit database, http://yann.lecun.com/exdb/mnist/

[2] K. Sato, N. Shimoda, Build your own machine-learning-powered robot arm using tensorflow and google cloud | Google Cloud blog, 2017.

[3] Keras documentation, https://keras.io/

[4] TensorFlow, https://www.tensorflow.org/

[5] A. Elfasakhany, E. Yanez, K. Baylon, R. Salgado, Design and development of a competitive low-cost robot arm with four degrees of freedom, Modern Mechanical Engineering, pp.47-55.

[6] OpenCV library document, https://opencv.org/

[7] K. Simonyan, A. Zisserman, Very deep convolutional networks for large-scale image recognition. Arxiv - Computer Vision and Pattern Recognition .

[8] S. Raschka, V. Mirajalili, Python machine learning (pp. 341-385).

[9] P. Bezak, P. Bozek, Y. Nikitin, Advanced robotic grasping system using deep learning, Procedia Engineering, 96, pp.10-20., 2014.

[10] A. Dhawan, A. Bhat, S. Sharma, H. K. Kaura, Automated robot with object recognition and handling features, International Journal of Electronics and Computer Science Engineering, ISSN- 2277-1956.

[11] E. B. Mathew, D. Khanduja, B. Sapra, B. Bhushan, Robotic arm control through human arm movement detection using potentiometers. 2015 International Conference on Recent Developments in Control, Automation and Power Engineering (RDCAPE), 2015.

[12] B.Iscimen, H. Atasoy, Y. Kutlu, S. Yildirim, E. Yildirim, Smart robot arm motion using computer vision, 2015.

[13] M.A. Jayaram, H. Fleyeh, Convex Hulls in Image Processing, A Scoping Review, American Journal of Intelligent Systems, 2016.

[14] N. Rai, B. Rai, P. Rai, Computer vision approach for controlling educational robotic arm based on object properties, 2nd International Conference on Emerging Technology Trends in Electronics, Communication and Networking. 2014

[15] T. S. Tonbul, M. Sarıtas, Beş eksenli bir edubot robot kolunda ters kinematic hesaplamalar ve yörünge planlaması. J. Fac. Eng. Arch. Gazi Univ. Vol 18, No 1, 145-167, 2013

[16] A. B. Rehiara, Kinematics of adeptthree robot arm, Robot Arms, ISBN: 978-953-307-160-2, 2011.

Optimization of Process Parameters of the Plate Heat Exchanger

Ceyda Kocabaş*‡, Ahmet Fevzi Savaş**,

*Quality Control in Manufacturing, Vocational School of Bilecik Şeyh Edebali University, Bilecik, Turkey

**Industrial Design, Bilecik Şeyh Edebali University, Faculty of Fine Arts and Design, Bilecik, Turkey

(ceyda.pak@bilecik.edu.tr, ahmetfevzi.savas@bilecik.edu.tr)

‡ Corresponding Author; Ceyda Kocabaş, Quality Control in Manufacturing, Vocational School of Bilecik Şeyh Edebali University, Bilecik, Turkey, Tel: +90 228 214 1620,

Fax: +90 228 214 1332,ceyda.pak@bilecik.edu.tr

Received: 17.01.2019 Accepted:17.03.2019

Abstract- The aim of this study is to determine the importance of the operational factors affecting the recovery performance in air-to-air heat recovery application where heat exchanger is used. The Taguchi experimental design method has been applied to show the effects of the factors and obtain the optimum process parameter combination. Thermal effectiveness has been determined as a performance characteristic. Experiments have been carried out at varying air flow rate, fresh and exhaust air inlet temperatures. Taguchi's $L_9(3^3)$ standard orthogonal array has been chosen as an experimental plan. The significance level of the control factors has been obtained by using analysis of variance (ANOVA). The results show that air flow rate is the most significant factor among the three factors that influences the thermal effectiveness. The results prove that Taguchi method is an easily applicable optimization tool for heat recovery systems.

Keywords Air to air heat recovery, plate heat exchanger, effectiveness, Taguchi method

1. Introduction

The energy policy of the world countries is focused on sustainability. Fossil-based fuels cause non-renewable sources are wasted day by day. The increase in consumption of these resources means more harm to the environment. There are various ways to reduce energy consumption, and one of them is to recover the waste heat. Especially, industrial systems that use high amounts of energy have a large heat recovery potential. By the way recovering and reusing of rejected heat instead of purchasing energy, waste heat recovery applications improve both efficiency and reduce energy costs [1].

There are several types of equipment that can be used for heat recovery. One of them is a heat exchanger. It is a device that can transfer the heat from one fluid to another at different temperatures in thermal contact. Usually, they are used in heating and cooling applications, such as space heaters, refrigerators and air conditioners. Plate type exchanger is one of the most widely used exchanger type for heat recovery. In this type, the two fluids are separated from each other by a thin plate and the heat transfer between the fresh and the exhaust fluid takes place without contacting each other.

The Taguchi method, one of the experimental design methods, can be used to determine which input factor influences the experimental result on what level and also obtain the optimum process parameter combination. Performance characteristics can be optimized through the setting of process design parameters and variability of a process can be reduced by selecting the optimal values of controllable factors. This method has been widely used nowadays because it lets to achieve desired results with less experimentation, in less time and with less cost. In addition, the optimum working conditions obtained from laboratory study can be reproduced at different times and also in different working environments.

Optimization studies for various heat exchangers are available in the literature. Jeom- Yul Yun and Kwan-Soo Lee [2] presented the determination of optimum values of the design parameters in a heat exchanger with a slit fin by using Taguchi method. The effects of the various design parameters

on the heat transfer and friction factor for the heat exchanger having enlarged and contracted oriented rectangular fins were analysed using the Taguchi method by Şahin et al.[3]. Yakut et al.[4] systematically analysed the effects of the various kinds of design parameters on the heat transfer and friction factor for heat exchangers having hexagonal fins using the Taguchi method. Qi et al. [5] determined five experimental factors affecting the heat transfer and pressure drop of a heat exchanger with corrugated louvered fins. The overall heat transfer, friction factor and the effect of the various design parameters on the heat transfer and friction factor for the heat exchanger equipped with square cross sectional perforated pin fins were investigated experimentally by Şahin and Demir [6]. Turgut et al. [7] studied the effect of the geometrical parameters on the performance of the concentric heat exchanger with injector turbulators using Taguchi experimental design method. Hsieh and Jang [8] optimized the parameters of louver finned-tube heat exchangers by the Taguchi method. Kotçioğlu et al. [9] invested experimentally the effects of six design parameters to reach minimum pressure drop and maximum heat transfer for a plate-fin type heat exchanger. An experimental study on a plate fin heat exchanger with navy fins has been conducted by Jungi et al. [10]. Jamshid et al. [11] carried out an experimental investigation to study the heat transfer characteristics in shell and helical tube heat exchangers by using of Wilson plot and Taguchi method. Du et al. [12] applied the Taguchi method to investigate the influence of various geometric parameters on heat transfer and flow resistance characteristics of overlapped helical baffled heat exchanger. Bilen et al. [13] studied the effect of flow rate, coil diameter and coil pitch on the heat transfer rate in plate type heat exchanger by the use of Taguchi Method.

As mentioned in the literature review, Taguchi optimization technique has been used in numerous studies, but the application of this method for the energy recovery based system has been scarce [1]. Another noteworthy difference is that previous investigations are mainly concerned with the optimization of geometric design parameters of exchangers. As different from previous experimental works, in the present study, optimization of the process design parameters of an air to air waste heat recovery application was achieved by means of Taguchi technique. The influence of three operating parameters on the thermal effectiveness was detailed. Contribution ratio and the optimum design value of each parameter was presented. By this way, the optimum combination of the parameters was determined. Differently, variance analysis (ANOVA) was applied to obtain the significance grade of the process parameters. The results of this study will be useful for designers who determine the parameters of the waste heat recovery process. And also these test data will expand the database of air to air heat recovery.

2. Experimental Set-Up

Schematic diagram of the heat recovery device used in the study is shown in Fig. 1. The working principle of the system is as follows: The fresh air passes through one side of the plates and at the same time the exhaust air passes through the other and heat transfer takes place. When the system starts to work, fresh air with a higher temperature than the outside air is given to the interior. The thermal energy load of the exhaust air is transferred to the fresh air by means of heat exchanger. [14,15]

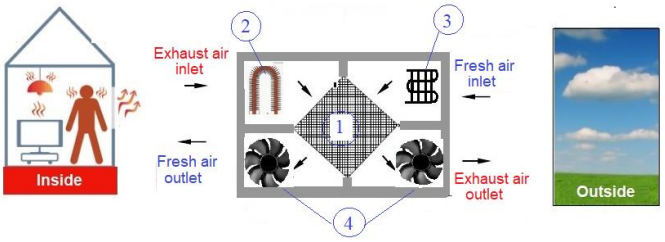

Fig. 1. Schematic display of the experimental apparatus: (1) heat exchanger, (2) heater, (3) evaporator, (4) fan.

The main components of the experimental apparatus were the heat exchanger, heater, evaporator, fans and data acquisition system. The outside of the test section was covered with a glass wool layer to provide insulation against heat loss to the surrounding air. The aluminium plate heat exchanger with 20 x 20 x 30 cm size was fitted in the center of the apparatus. The photo and geometric dimensions of the heat exchanger were shown in previous studies [14, 15].

Fresh and exhaust air were used as working fluids. The tests were carried out at different values for air flow rate, fresh and exhaust air inlet temperatures. For this purpose, the waste heat recovery system was designed with two 2500/2700 RPM fans, one to suck exhaust air and the other to blow fresh air. An anemometer was used in to determine the velocity of the air flow entering into the system and the speed of the fans was adjusted by using a single-phase speed controller. Lamellar resistance heaters were used to get hot air and air compressor cooling apparatus was used to get cold air. The inlet and exhaust air temperatures were set to different temperatures by means of digital thermostats. The devices and their accuracies are given in Table 1.

Table 1. Uncertainty of measurement devices

3. Materials and Methods

Measurement Device	Name	Range	Accuracy
Anemometer	Prova AVM-07	0-45/ m/s	± 3%
Thermostat	Emko ESM-3710	(-40) / (+85) °C	± 1%
Thermostat	Evko EVKB 21	(-50) / (+130) °C	± 1%

3.1. Heat Transfer

In this experimental work, thermal effectiveness (efficiency) has been selected as the performance statistic. Pressure drop and latent heat transfer were neglected and it was assumed that there was no heat loss to the external atmosphere. The thermal effectiveness can be defined as the ratio of the actual heat transfer to the maximum possible heat transfer. Thermal effectiveness is calculated by the following equation (1) [10, 15]:

$$\varepsilon = Q/Q_{max} \quad (1)$$

The amount of actual heat transferred can be found from the heat given by the hot fluid or taken from the cold liquid:

$$Q = C_h(T_{hi} - T_{ho}) \text{ or } \quad Q = C_c\,(T_{co} - T_{ci}) \quad (2)$$

$$C_h = \dot{m}_h C_{ph} \quad (3)$$

$$C_c = \dot{m}_c C_{pc} \quad (4)$$

$$Q_{max} = \; C_{min}\,(T_{hi} - T_{ci}) \quad (5)$$

The Q_{max} can be defined as the maximum amount of heat transfer can be possible. This value can be found by selecting the smaller of the C_h and C_c and multiplying it with the difference between the inlet temperatures of the cold and hot fluids. For further information, previous studies can be reviewed [14-15].

3.2. Application of Taguchi Method

When the number of process parameters increases, it is necessary to carry out a large number of experiments. Taguchi approach presents experimental plans that simplify and standardize these experiments. The objective of this method is acquiring data in a controlled way and thus, getting information about the behavior of the process [16]. Taguchi's method is based on an orthogonal array, and some of the advantages that these arrays offer to designers are: influence of multiple controllable factors on the quality characteristics and the variations can be analyzed, optimum parametric combinations can easily be found out [1]. Also, the maximum and minimum value ranges of the results of untested experiments can be estimated using this technique [17]. For these reasons, this approach has been applied in a wide variety of fields.

According to Taguchi, process performance is influenced by both controllable and uncontrollable factors. Variables such as part size, fluid temperature, material type, flow rate, and electric current are called controllable factors and the levels can be selected by the researchers. On the other hand, variables that are difficult to control, such as moisture, noise, vibration, dust, product wear, are called uncontrollable factors [18]. The main focus of the Taguchi method is to determine the optimal levels of controllable factors and to reduce the variability that derives from uncontrollable factors. Thus, it is possible to take precautions against the factors that cause variation before the production begins [6].

The signal-to-noise ratio (S/N) has been developed as a basic statistical criterion for evaluating performance indicators in the Taguchi approach [12]. The signal(S) is also called as controllable factor and represents the actual value taken from the system. The noise (N) is called as uncontrollable factor and represents the proportion of undesired factors in the test result [19]. There are some S/N ratios available depending on the type of performance characteristic: "Larger is better", "lower is better" and "nominal is best". Regardless of which S/N ratio is used, the larger S/N ratio is always selected. Because the Taguchi technique aims to keep to minimize the effects of uncontrollable factors (N) while maximizing the effects of controllable factors (S)[7]. The S/N ratio can be calculated by using the data in the test sample array. The objective of this study is the maximization of thermal effectiveness, which has been determined as a performance characteristic. For this purpose, "Larger is better" was selected and so S/N ratio was evaluated by using the following equation:

$$S/N = -10\log\left[\frac{1}{n}\sum_{i=1}^{n}\frac{1}{y_i^2}\right] \quad (6)$$

In the given equation, y is the calculated value of the performance characteristic and n is the number of experiments carried out under these experimental conditions. ANOVA can be performed to obtain statistics of the calculated S / N values and to determine which experimental factor influences the test result at what level [19].

4. Results and Discussion

In the present work, three factors were selected related to the heat transfer characteristic. These factors are fresh air inlet temperature, air flow rate and exhaust air inlet temperature. Three levels determined for each factor are presented in Table 2.

Table 2. Factors and levels

	Factors	Level 1	Level 2	Level 3
A	Fresh air inlet temperature	0 °C	5 °C	10 °C
B	Air flow rate	1,2 m/s	1,6 m/s	2 m/s
C	Exhaust air inlet temperature	28°C	34°C	40°C

Table 3. Confirmation test

Optimum Levels			
Effective Factors	Level	Value	Average S/N
Fresh air inlet temperature	1	0 °C	30,95
Air flow rate	1	1,2 m/s	31,16
Exhaust air inlet temperature	3	40 °C	31,06
Mean of S/N ratios	30,863		
	Expected		Actual
Expected S/N ratio	31,44		31,36
Optimum effectiveness value	37,34		37

If the traditional experimental method had been used, it would have been necessary to perform 3^3= 27 experiments to test all factors and levels. In this study, Taguchi method was implemented and the L_9 (3^3) orthogonal array was selected as experimental plan. Thus, the number of experiments that need to be done was reduced to 9. The L_9 orthogonal array used for

the experiments is given in Table 4. The numbers 1, 2, and 3 on each line indicate the levels of the factors.

Table 4. The orthogonal array L_9 (3^3)

Experiment No	FACTORS AND LEVELS		
	A	B	C
	Fresh air inlet temp. (°C)	Air flow rate	Exhaust air inlet temp. (°C)
1	1	1	1
2	1	2	2
3	1	3	3
4	2	1	2
5	2	2	3
6	2	3	1
7	3	1	3
8	3	2	1
9	3	3	2

L_9 test plan prepared in accordance with the L_9 orthogonal array is given in Table 4. As can be seen from this table, 9 different experiments would be implemented using combinations of the three factors selected at different levels. Other factors were kept constant. Thermal effectiveness ε was taken as the signal factor and the noise factor was ignored. Each experiment was repeated twice under the same conditions at different times in order to detect the effect of noise sources on the heat transfer. Statistical and graphical analyses were performed with the Minitab software program.

The average S/N values obtained for each experiment are presented in Table 5 and the S/N ratio of every factor in every level is given graphically in Fig. 2. As mentioned above, S/N values can help researchers to determine the effect of parameters. The greatest S/N values at all levels of the parameters provide optimum performance. Considering Fig. 2, S/N ratio decreases by increasing fresh air inlet temperature and air flow rate and also increases by increasing exhaust air inlet temperature. Recent studies proved that heat exchanger effectiveness decreased as the air flow rate increased [15, 20-23] Mardiana and Rıffat [20] stated that; reducing air flow rate always increases efficiency in any heat recovery system and the effectiveness is decreased with increasing inlet fresh temperature [24]. The following values can be selected as the optimum parameters: 0 °C (A_1), the first level of fresh air inlet temperature; 1.2 m/s (B_1), the first level of air flow rate and 40 °C (C_3), the third level of exhaust air inlet temperature. $A_1B_1C_3$ has the largest S/N ratio, that's why this can be defined as the optimum parameter combination for this study.

Table 5. S/N ratios

Experiment no	Factors			Effectiveness	S/N
	A	B	C		
	Fresh air inlet temp. (°C)	Air flow rate (m/s)	Exhaust air inlet temp. (°C)		
1	0	1,2	28	35,8	31
2	0	1,6	34	35	31
3	0	2	40	35	31
4	5	1,2	34	36,1	31
5	5	1,6	40	35,7	31
6	5	2	28	33,4	30
7	10	1,2	40	36,5	31
8	10	1,6	28	33,6	31
9	10	2	34	33,4	30

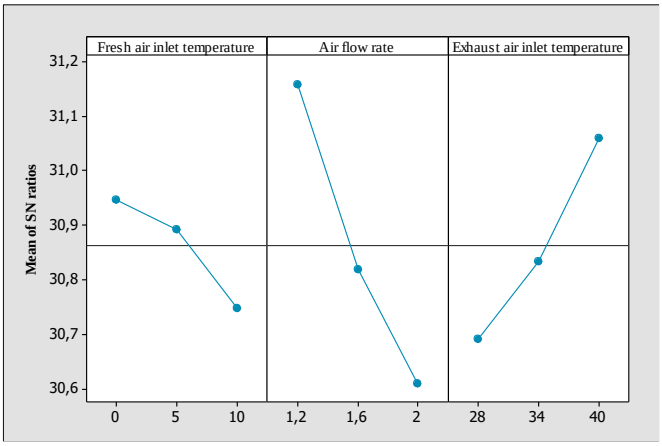

Fig. 2. Main effects plot for SN ratios

Following, the analysis of variance (ANOVA) is used to evaluate the experimental data. This statistical method makes the analysis results more significant and reliable [12]. ANOVA is frequently used to determine how the parameters affect the targeted performance characteristic and how the different levels of parameters change this effect. ANOVA was performed using the S/N ratios given in the Table 5. For this analysis, the mean of the S / N ratios is separately taken to determine the effect of each level of the factors. For example, if the first level (0 °C) of the fresh air inlet temperature is selected, 1, 2 and 3 numbered experiments of Table 5 must be taken into account. Then, the S/N ratio average is determined as (31,08+30,88+30,88) /3 = 30,95. When the first level (1,2 m/s) of the air flow rate is selected, 1, 4 and 7 numbered experiments of Table 5 must be taken into account. The S/N ratio average is calculated as (31,08+31,15+31,25) /3 = 31,16. As the first level (28 °C) of the exhaust air inlet temperature is selected, 1, 6 and 8 numbered experiments of Table 5 must be taken into account. The S/N ratio average is found as (31,08+30,47+30,53) /3 = 30,69. The mean of the S/N ratios of other levels of each factor was calculated in this way. These calculations are shown in Table 6. To find out the mean of all S / N ratios, the arithmetic average of the 9 values shown in bold is found. As a result, the mean of the S / N ratios is determined as 30,863.

For ANOVA, Sum of squares of the total, which indicates the total variance of the S/N ratio, needs to be evaluated [25]. The SS_T value is the sum of squares of SS_A, SS_B and SS_C

which are the sum of squares of individual factors, and the sum of squares of error (SS_e). The sum of the squares was calculated by the following formulas [12, 26]:

Sum of the squares for total:

$$SS_T = \sum_{i=1}^{n} (\eta_i - \eta_m)^2 \quad (7)$$

Sum of the squares for factor A:

$$SS_A = n_{A_i} \sum_{i=1}^{k_A} (\eta_{A_i} - \eta_m)^2 \quad (8)$$

Sum of the squares for error:

$$SS_E = SS_T - \sum_{i=A}^{E} SS_A \quad (9)$$

η_i = S/N ratio

η_m =mean of S/N ratios

n = total number of experiments

k_A = number of levels of factor A

n_{A_i} = number of experiments at level i of factor A

η_{A_i} = S/N value at level i of factor A

The sum of the squares of all factors was calculated by this way and the ANOVA results are given in Table 7. For instance; the sum of the squares for the factor A (fresh air inlet temperature) is determined as: $SS_A = [(3 * (30{,}95 - 30{,}863)^2 + 3 * (30{,}89 - 30{,}863)^2 + 3 * (30{,}75 - 0{,}863)^2] = 0{,}0626$.

Table 6. The mean of S/N ratios

Fresh air inlet temperature				Air flow rate				Exhaust air inlet temperature		
Level 1	*Level 2*	*Level 3*		*Level 1*	*Level 2*	*Level 3*		*Level 1*	*Level 2*	*Level 3*
31,08	31,15	31,25		31,08	30,88	30,88		31,08	30,881	30,881
30,88	31,05	30,53		31,15	31,05	30,47		30,47	31,15	31,053
30,88	30,47	30,47		31,25	30,53	30,47		30,53	30,474	31,245
30,95	**30,89**	**30,75**		**31,16**	**30,82**	**30,61**		**30,69**	**30,84**	**31,06**
									Mean of S/N ratios	30,863

Degree of freedom of every column is derived from the levels of each control factor minus 1. The sum of the mean squares (MS) was calculated by dividing the sum of squares (SS) of each factor by the degrees of freedom (DF) of that factor [12]. The rank row is the order of factors according to their significance. The contribution ratio of each factor can be evaluated separately using the ANOVA table.

Contribution ratio means the effect of factor on the performance characteristic and it can be found out dividing the sum of the square of this factor by the total. For example, contribution ratio for fresh air inlet temperature (factor A) can be calculated as 0.0626 / 0.7263 = 0.086 (8,6 %). Contribution ratios of each factor are shown graphically in Fig.3.

Table 7. ANOVA table

	Degree of freedom (DF)	Average values			Sum of squares (SS)	Sum of mean squares (MS)	Contribution ratio %	Rank
		Level 1	Level 2	Level 3				
Fresh air inlet temperature	2	30,95	30,89	30,75	0,0626	0,0313	8,6	3
Air flow rate	2	31,16	30,82	30,61	0,4577	0,2289	63	1
Exhaust air inlet temperature	2	30,69	30,84	31,06	0,2055	0,1028	28,3	2
Error	2				0,00046	0,000234	0,1	
Total	8				0,7263		100	

The air flow rate has 63% of total effect, as it can be seen from Fig. 3 and Table 7. This means the parameter B is the most significant factor in heat recovery. The inlet temperature of the exhaust air is the secondary effective factor with the ratio of 28% and the fresh air inlet temperature was the factor with the lowest effect on the result of the experiment with a ratio of 8%. Results are compatible with database and literature. Mardiana and Riffat [20] specified that: air flow rate has a significant effect on all types of heat recovery efficiency or recovered heat and the temperature of the inlet air has a minor influence in the heat recovery system for both sensible and total efficiency. Niu and Zhang [24] submitted that sensible effectiveness does not change much with supply air inlet temperature. Yaici et al. [27] indicated that the outdoor temperature has only minor effects on heat recovery.

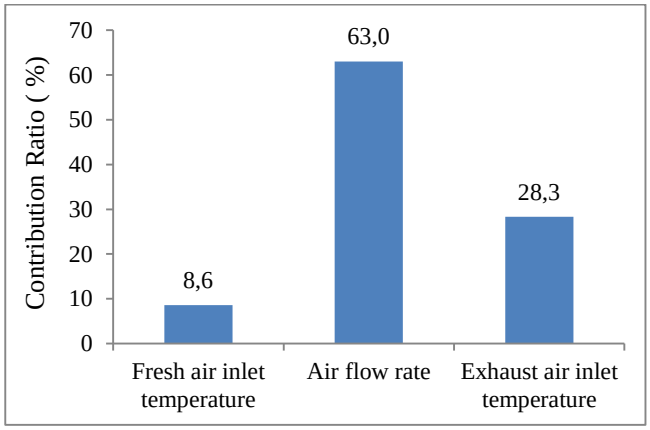

Fig. 3. Contribution ratios

After the ANOVA was carried out, the confirmation tests should be performed on the optimum parameter values. For this purpose, the optimum process parameters are selected. The second step is to predict and verify the improvements of the performance characteristic [7]. The test sample was prepared for optimal conditions ($A_1B_1C_3$). The results of the confirmation test are shown in Table 3. In order to test the predicted results, confirmation experiments were conducted within 95% significance level confidence (5% error). In order to find the expected S/N ratios following equation can be used [26]:

$$\hat{\eta} = \eta_m + \sum_{i=1}^{k} (\bar{\eta}_i - \eta_m) \quad (10)$$

$\hat{\eta}$ = expected S/N ratio

η_m = mean of S/N ratios

$\bar{\eta}_i$ = average S/N ratio at the optimum level

k = number of important factors affecting the performance

Since all three factors were determined as significant in the above analysis, each factor needs to be included in the calculation. By using the above equation, the expected S/N ratio was found 31,44 and the optimum effectiveness was found 37,34. The actual and expected S/N ratio and effectiveness values are shown comparatively in Table 3. When Table 3 is examined, it is observed that the expected and actual values are quite compatible with each other. And also results presents, the determined optimum process parameter shows better performance than the previous observations. Confirmation results proved the validity and reliability of the Taguchi approach used in the optimization of parameters.

5. Conclusion

In this article, the influence of various process parameters on waste heat recovery performance of plate heat exchanger was investigated experimentally. A device was installed in a laboratory environment where air to air waste heat recovery was enabled by means of a cross-flow plate-fin heat exchanger. The fresh air inlet temperature, the air flow rate and the exhaust air inlet temperature were determined as operating parameters. Three levels were selected for each parameter. Thermal effectiveness ε was taken as the performance indicator. The influence of three operating parameters on the thermal effectiveness was analysed. The optimum process conditions were determined by using the Taguchi method. The experiments were planned in accordance with Taguchi's L_9 orthogonal array and each trial was performed under different conditions of air flow rate, fresh and exhaust air inlet temperatures. The factors and levels were examined by using the signal-to-noise ratios and ANOVA methods. Minitab statistical software program was used for analysis. Results indicate that higher effectiveness can be achieved at a low fresh air inlet temperature, low air flow rate and high exhaust air inlet temperature. Based on the ANOVA results, all control factors have a significant impact on the quality characteristic. The most significant parameter has been found as air flow rate (63%). The second parameter is the exhaust air inlet temperature (28%) and the last one is the fresh air inlet temperature (8%). The optimum process parameter combination has been obtained as (A_1, B_1, C_3). At the end of the study, the validity of the Taguchi method was tested by performing the confirmation test. Compared the other trials, the highest thermal effectiveness (37%) is achieved when the optimum parameter combination is used. The results show that the Taguchi approach can be used to improve the effectiveness of air-to-air recovery. The predicted and experimental results are in very good agreement with each other. This show, the optimum conditions determined by the Taguchi method can be used reliably for real heat recovery applications.

Abbreviations

c	cold air
h	hot air
hi	hot air inlet
ci	cold air inlet
co	cold air outlet
ho	hot air outlet
$\dot{m}$	mass flow
C_{ph}	specific heat of the hot air
C_{pc}	specific heat of the cold air

References

[1] S. Coşkun, A. R. Motorcu, N. Yamankaradeniz, E. Pulat, "Evaluation of control parameters' effects on system performance with Taguchi method in waste heat recovery application using mechanical heat pump", Refrigeration, vol. 35, pp. 795-809, 2012.

[2] J. Yun and K. Lee, "Influence of design parameters on the heat transfer and flow friction characteristics of the heat exchanger with slit fins", International Journal of Heat and Mass Transfer, vol. 43, pp. 2529-2539, 2000.

[3] B. Şahin, K. Yakut, I. Kotcioğlu, C. Çelik, "Optimum design parameters of a heat exchanger", Applied Energy, vol. 82, pp. 90–106, 2005.

[4] K. Yakut, N. Alemdaroğlu, B. Şahin, C. Çelik, "Optimum design-parameters of a heat exchanger having hexagonal fins", Applied Energy, vol. 83, pp. 82–98, 2006.

[5] Z. Qi, J. Chen, Z. Chen, "Parametric study on the performance of a heat exchanger with corrugated louvered fins", Applied Thermal Engineering, vol. 27, pp. 539–544, 2007.

[6] B. Şahin and A. Demir, "Performance analysis of a heat exchanger having perforated square fins", Applied Thermal Engineering, vol. 28, pp. 621-632, 2008.

[7] E. Turgut, G. Çakmak, C. Yıldız, "Optimization of the concentric heat exchanger with injector turbulators by Taguchi method", Energy Conversion and Management, vol. 53, 268–275, 2012.

[8] C.T. Hsieh and J.Y. Jang, "Parametric study and optimization of louver finned-tube heat exchangers by Taguchi method", Applied Thermal Engineering, vol. 42, pp. 101-110, 2012.

[9] I. Kotcioglu, A. Cansiz, M. N. Khalaji, "Experimental investigation for optimization of design parameters in a rectangular duct with plate-fins heat exchanger by Taguchi Method", Applied Thermal Engineering, vol. 50, pp. 604-613, 2013.

[10] D. Junqi, Z. Yi, L. Gengtian, X. Weiwu, "Experimental study of wavy fin aluminium plate fin heat exchanger", Experimental Heat Transfer, vol. 26, pp. 384–396, 2013.

[11] N. Jamshidi, M. Farhadi, D.D. Ganji, K. Sedighi, "Experimental analysis of heat transfer enhancement in shell and helical tube heat exchangers", Applied Thermal Engineering, vol. 51, pp. 644-652, 2013.

[12] T. Du, W. Du, K. Che, L. Cheng, "Parametric optimization of overlapped helical baffled heat exchangers by Taguchi method", Applied Thermal Engineering, vol. 85, pp. 334-339, 2015.

[13] K. Bilen, S. Yapıcı, C. Çelik, "A Taguchi approach for investigation of heat transfer from a surface equipped with rectangular blocks", Energy Conversion and Management, vol. 42, pp. 951-961, 2001.

[14] C. Kocabaş, "Experimental analysis of waste heat recovery performance of plate exchangers manufactured from different materials", Master's Thesis, Bilecik Seyh Edebali University, Institute of Science, 2014.

[15] C. Kocabaş and A.F. Savaş, "Comparison of waste heat recovery performances of plate-fin heat exchangers produced from different materials", Contemporary Engineering Sciences, vol. 8(11), pp. 453 – 466, 2015.

[16] I. Kotcioglu, M. N. Khalaji , A. Cansiz, "Heat transfer analysis of a rectangular channel having tubular router in different winglet configurations with Taguchi method", Applied Thermal Engineering, vol. 132, pp. 637-650, 2018.

[17] C. Danışman, "Experimental analysis on efficiency of a plate heat exchanger" [In Turkish], Master of Thesis, Institute of Science and Technology, 2010.

[18] Ö. Tan and A. Ş. Zaimoğlu, "Investigation of effects to the rheological properties of additive materials which are used on cement enjections" [In Turkish], Pamukkale University Engineering College Journal of Engineering Science, vol. 10(2), pp. 275-281, 2004.

[19] G. Taguchi and Y. Wu, Taguchi Methods Case Studies from the US and Europe, American Supplier Institute Inc., Michigan, 1989.

[20] A. Mardiana and S. B. Riffat, "Review on physical and performance parameters of heat recovery systems for building applications", Renewable and Sustainable Energy Reviews, vol. 28, pp. 174-190, 2013.

[21] A. Mardiana- Idayu and S. B. Riffat, "An experimental study on the performance of enthalpy recovery system for building applications", Energy and Buildings, vol. 43(9), pp. 2533-2538, 2011.

[22] Y.E. Fouih, P. Stabat, P. Rivière, P. Hoang, V. Archambault, "Adequacy of air-to-air heat recovery ventilation system applied in low energy buildings", Energy and Buildings, vol. 54, pp. 29-39, 2012.

[23] M. Nasif, R.AL-Waked, G. Morrison, M. Behnia, "Membrane heat exchanger in HVAC energy recovery systems, systems energy analysis", Energy and Buildings, vol. 142, pp. 1833-1840 ,2010.

[24] J.L. Niu and L.Z Zhang, "Membrane-based Enthalpy Exchanger: material considerations and clarification of moisture resistance", Journal of Membrane Science, vol. 189, pp. 179-191, 2001.

[25] E. Turgut and A. Dikici, "Optimization of design parameters of co-axial heat exchanger with taguchi method" [In Turkish], 6th International Advanced Technologies Symposium, 05, 2011, pp. 278-281.

[26] M. Savaşkan, Y. Taptık, M. Ürgen, "Performance optimization of drill bits using design of experiments" [In Turkish],, İtu Article, Engineering, vol. 3(6), pp. 117-128, 2004.

[27] W. Yaïci, M. Ghorab, E. Entchev, "Numerical analysis of heat and energy recovery ventilators performance based on CFD for detailed design", Applied Thermal Engineering, vol. 51, pp. 770-780, 2013.

A Sampling About For Economic Pipe Diameter Calculation

Enes Kalyoncu*‡

* Department of Machinery, Vocational School of Gelisim, Istanbul Gelisim University, Istanbul, Turkey

(ekalyoncu@gelisim.edu.tr)

‡Corresponding Author; Enes Kalyoncu, Department of Machinery, Vocational School of Gelisim, Istanbul Gelisim University, Istanbul, Turkey, Tel : +90 212 422 70 00

Fax : +90 212 422 74 01, ekalyoncu@gelisim.edu.tr

Received: 10.03.2018 Accepted:25.01.2019

Abstract- Pumps are widely used in our homes, in buildings, in industrial applications, in agriculture, in water supply and many other applications, even though we are not aware of them. When designing a pump system, it is necessary to compare different solutions to choose the most efficient and efficient system. To find the most intelligent solution, some basic facts must be revealed. As a result of the experimental work done, the loss coefficients are calculated with the aid of the determined pressure deductions taking into consideration the flow direction for the flat pipes, valves and fittings (elbows, nipples, cuffs, record, curve, reduction and TE (transitional elements) It was calculated and presented in tables. In this study, a program was developed to determine the optimum diameters of the pipes that allow the water from the plant to be transported at a certain distance. Galvanized pipes were used in the study. The least-lost diameters and the lowest economic costs were calculated for these pipes.

Keywords : Centrifugal pump, diameter calculation, pipe losts, economic pipe diameter.

1. Introduction

Pumping systems account for nearly 20% of the world's electrical energy demand and range from 25-50% of the energy usage in certain industrial plant operations[1]. Pumping systems are widespread; they provide domestic services, commercial and agricultural services, municipal water/wastewater services, and industrial services for food processing, chemical, petrochemical, pharmaceutical, and mechanical industries[1]. The initial setup and operating costs of these systems are important parameters that the account must participate in designing and operating the system[6]. Although pumps are typically purchased as individual components, they provide a service only when operating as part of a system. The energy and materials used by a system depend on the design of the pump, the design of the installation, and the way the system is operated. These factors are interdependent. What's more, they must be carefully matched to each other, and remain so throughout their working lives to ensure the lowest energy and maintenance costs, equipment life, and other benefits. The initial purchase price is a small part of the life cycle cost for high usage pumps. While operating requirements may sometimes override energy cost considerations, an optimum solution is still possible[1].

When designing a pump system, it is useful to compare different solutions to choose the most efficient and efficient system. To find the most intelligent solution, some basic facts must be revealed[12]. Over the past decade, the world has been focusing on lifetime cost (PPM) in pump selection. The aim is that when buying a pump, it is not only the purchase price, but the lifetime cost of the pump is important. Purchasing, operation and maintenance within the lifetime cost, cost of production loss in case of failure as much as the cost of energy, cost of dismantling are included[7]. Pump selection is primarily determined by the specification of operating conditions – in other words, the operating properties the pumps will be supplied for. The operating conditions primarily comprise data on the fluid handled (e.g. temperature, density, viscosity, dry substance content, sand content or other substances in the fluid), the expected flow rate and the required head, the suction behaviour and the speed of the centrifugal pump. Also required is information on the drive size and rating, the operating mode, the expected frequency of starts as well as any factors determined by the system or environmental regulations such as the maximum permissible noise emission, permissible vibrations, pipeline forces and potential explosion hazards[4].

2. Centrifugal Pumps

The capacity (flowrate, discharge, or Q) of a pump is the volume of liquid pumped per unit of time, usually measured in SI units in cubic meters per second for hour for small pumps [2]. The functionality and performance of a pump strongly depends on its hydrodynamics [13].

When centrifugal pumps are operated at constant speed, their flow rate Q increases as their head H decreases. In the characteristic head versus flow curve, also referred to as H/Q curve, the head H is plotted against the flow rate Q [4].

Proper pumping system design is the most important single element in minimizing [1]. The most challenging aspect of the design process is cost-effectively matching the pump and motor characteristics to the needs of the system. This process is often complicated by wide variations in flow and pressure requirements [3].

The piping diameter is selected based on the following factors:

• Economy of the whole installation (pumps and system)

• Required lowest flow velocity for the application (e.g., avoid sedimentation)

• Required minimum internal diameter for the application (e.g., solids handling)

• Maximum flow velocity to minimize erosion in piping and fittings

• Plant standard pipe diameters

Decreasing the pipeline diameter has the following effects:

• Piping and component procurement and installation costs will decrease [1].

• Pump installation procurement costs will increase as a result of increased flow losses with consequent requirements for higher head pumps and larger motors. Costs for electrical supply systems will therefore increase [1].

• Operating costs will increase as a result of higher energy usage due to increased friction losses [1].

3. Optimum Pipe Diameter Calculation

As a method in the study, a program was written by using the flow in the pipe, the flow friction losses and the heat transfer equations. Various results have been obtained for optimum selection of system components by calculating optimum pipe and insulation thicknesses in different pipe types, various insulation pedestals. The following formula and equations are used to calculate the flow and heat transfer in the pipe in the related program [6].

The pipeline system with a total length of 2400 m and the pump will be transported to a settlement of 1950 people at a height of 260 m. Daily water consumption per person is 250 lt. The pump to be used in the installation is required to work 2.5 hours a day. The pumps to be used in the pipeline are the pipes selected from the pipe catalog of a company and their products are selected as "Galvanized Threaded Pipe" according to DIN 2440 norm. An economic pipe diameter account will be made for a life of 20 years. Galvanized steel pipes are often used for water cooling systems both in industrial plants and in domestic buildings [14].

The project was carried out with reference to Ibrahim Gentez- economic pipe diameter account booklet.

L : pipeline length : 2400 m

Q : flow : 250 tl / (day * person)

Hg : 260 m

tp : pump run time : 2,5 hour / day

Person number : 1950

n (Project life) : 20 year

g (gravity) : 9,81 m/s^2

µg : engine efficiency : %75 (0,75)

electricity costs : 0,087 $ / kWh (Low Voltage - Single Time - unit prices for 1 kWh with tax January,2019) [8].

Table 1 Pipe specifications and price [9].

Diameter	Rated Diameter (DN)	Outside Diameter (mm)	Wall (mm)	Pipe Unit Price($)
½”	15	21,3	2,65	2,070
¾”	20	26,9	2,65	2,701
1”	25	33,7	3,25	3,902
1 ¼”	32	42,4	3,25	5,006
1 ½”	40	48,3	3,25	5,767
2”	50	60,3	3,65	8,059
2 ½”	65	76,1	3,65	10,355
3”	80	88,9	4,05	13,463
4”	100	114,3	4,50	19,773
5”	125	139,7	4,85	26,716
6”	150	165,1	4,85	31,769

Calculation of all desired values for nominal diameter 15.

3.1. Calculation Of Internal Diameter

Di: Inner diameter

Do: outer diameter

Wall (t): wall diameter

Di = Do – 2*t

Di = 21, 3 – 2*2, 65 = 16 mm

3.2. Calculation Of Flow (Q)

$$Q=\frac{250\ lt}{dailyxperson}*\frac{1\ daily}{2{,}5\ hours}*\frac{1\ hour}{3600\ sc}*1950 person*\frac{1m3}{1000\ lt}$$

Q = 0,0542 m^3/s = 195 m^3/h (the same value will be used in all diameters).

3.3. Vort (Average Speed) Calculation

$$Vort=\frac{4*Q}{\pi*(Di)^2}=\frac{4*0{,}0542 m^3/s}{\pi*(0{,}016m)^2}=269{,}403\frac{m}{s}$$

3.4. Reynolds Number of Fluid (Re)

µ (kinematic viscosity) = 1,005* 10$^{(-6)}$ m^2/s

$$Re=\frac{Vort*Di}{\mu}=\frac{(269{,}403\ m/s)*0{,}016\ m}{1{,}005*10^{-6}m^2/s}=4289001{,}369$$

3.5. Λ (conductivity) Calculation of Value

Ɛ= Equivalent roughness ratio = 0,15 * 10^{-3}

$$\Lambda=\frac{1{,}325}{[\ln(\frac{\varepsilon}{3{,}7*Di}+\frac{5{,}74}{\mathrm{Re}^{0{,}9}})]\text{^}2}=\frac{1{,}325}{\left[\ln\left(\frac{0{,}15*10^{-3}}{3{,}7*0{,}016}+\frac{5{,}74}{(4{,}289*10^{6})^{0{,}9}}\right)\right]^2}=$$

0,0372

3.6. "J" Flat Tube Energy Loss That Occurs At Unit Size

$$j=\frac{\Lambda*\mathrm{Vort}^2}{2*\mathrm{Di}*\mathrm{g}}=\frac{0{,}0371*\left(269{,}403\frac{m}{s}\right)^2}{2*0{,}016*9{,}81m/s^2}=8578{,}999mss/m$$

3.7. Hk Straight Pipe Loss Calculation

Equipment/instruments especially that create a high-pressure drop and are provided with a bypass line (to have the facility for maintaining process continuity even during maintenance work). i.e. plate heat exchangers, control valves, etc. are provided with a bypass arrangement, which normally has two isolation valves in line of the unit and a flow regulation valve in parallel to this unit. In normal operations, as fluid passes through the main units either the plate heat exchanger or control valve, it exerts an additional pressure drop. Accordingly, the supply pressure for the fluid stream is estimated, which the connecting unit like the centrifugal pump creates. The centrifugal pump is selected based on this created pressure drop by the unit. During bypassing of the connected unit, this additional pressure is eliminated, while running pump discharges the high flow rate as per the typical pump characteristics. To avoid this situation, it is always recommended to use a lower size bypass line with a regulation valve to create pressure equivalent to the main connecting unit [10]. The amount of pipe losses of a private company is shown on the chart.

Hk=J*L=8578,999 mss/m*2400 m=20859597,569 mss

Table 2 Equipment used in installation and loss coefficient value [15].

Equipment	K	Adet	K*Adet
Klope+Strainer	10	1	10
E/xpansion Option	0,4	1	0,4
Shrinkage Element	0,012	1	0,012
Storage Entry	1	1	1
Valve	0,19	1	0,19
Check Valve	2,5	1	2,5
90° Elbow	1,12	3	3,36
Sleeve	0,06	400	24
		ΣK	41,462

One pipe size: 6 m

Total pipeline length: 2400

$\frac{2400}{6}$ =400 Pipes to be used

The K loss coefficient values given in the respective tables for each element that cause the loss of local energy that we can find to test are determined by the average value, which is a criterion emphasizing the loss of energy by the manufacturer firm [5].

3.8. H_L Calculation of Local Losses

$$\mathrm{HL}=\ \Sigma k*\frac{Vort^2}{2*g}=41{,}462*\frac{\left(269{,}403\frac{m}{s}\right)^2}{2*9{,}81\frac{m}{s^2}}=153375{,}423\ \mathrm{mss}$$

3.9. Hm Calculation of Energies to be Supplied to the System

Hm=Hk + HL + Hg =20589597,569 mss + 153375,426 mss + 260m =20743232,991 mss

3.10. Ne Calculation of Effective Power

γ=9810N/m^3

$$Ne=\frac{\gamma*Q*Hm}{\mu g}*\frac{1kW}{1000W}=\frac{9810\frac{N}{m^3}*\frac{0{,}0542m^3}{s}*20743232{,}991}{0{,}75}*\frac{1kW}{1000W}=14696580{,}574\ kW$$

3.11. Nm Calculation of Engine Power

α: Safety Factor

Ne ≥34 kW α : 1,1

34 kW ≥ Ne ≥6 kW α : 1,2

Ne ≤ 6,2 kW α : 1,3

Nm=α * Ne =1,1 * 146696580,574

Nm=16166238,632 kW

3.12. Calculation of Annual Electricity Costs (A.E.C.)

Energy Market Regulation Board Cost: 22, 1093 penny/kWh [8]

$$\mathrm{A.}E.\mathrm{C.}=Nm\ *\ T\ *\ \mathrm{Fee}\ =16166238{,}632*\frac{2{,}5\ hour}{1\ day}*\frac{365{,}25\ day}{1\ year}*0{,}36\frac{\$}{kWh}=531424679{,}273\ \$/year$$

3.13. Calculation of Annual Fixed Cost (A.F.C.)

i: Percentage increase in pipe unit price %15 (0,15)

n : project life 20 years

k : capital repayment factor

$$k=\frac{i*(i+1)^n}{(i+1)^n-1}=\frac{0{,}15*1{,}15^{20}}{1{,}15^{20}-1}=0{,}159$$

A.F.C= Pipe unit price * k =2,070*0,159 = 0,330697184 $/(year * m)

3.14. Annual Total Fixed Cost Calculation (A.T.F.C.)

A.T.F.C. = A.F.C. * L =0,330697184 $/(year*m) * 2400 m = 793,6732405 $/year

3.15. Annual Total Cost Calculation (A.T.C.)

Total cost consists of two components; investment and operating cost.

A.T.C. = A.T.F.C. + A.E.C. =793,6732405 + 5314246794,273 = 5314246795066,20 $/year

4. Unit Energy Costs And Optimum Diameters

Table 3 Calculation of whole desired values for all nominal diameter

Diameter	out diameter	wall	Price($)	Inner diameter	Flow rate	Vort	Re
15	21,3	2,65	2,070	0,016	0,0542	269,4029	4289001,37
20	26,9	2,65	2,701	0,0216	0,0542	147,8205	3177038,05
25	33,7	3,25	3,902	0,0272	0,0542	93,2190	2522941,98
32	42,4	3,25	5,006	0,0359	0,0542	53,5123	1911532,64
40	48,3	3,25	5,767	0,0418	0,0542	39,4720	1641723,01
50	60,3	3,65	8,059	0,053	0,0542	24,5522	1294792,87
65	76,1	3,65	10,355	0,0688	0,0542	14,5702	997442,18
80	88,9	4,05	13,463	0,0808	0,0542	10,5638	849307,20
100	114,3	4,5	19,773	0,1053	0,0542	6,2199	651700,11
125	139,7	4,85	26,716	0,13	0,0542	4,0809	527877,09
150	165,1	4,85	31,769	0,1554	0,0542	2,8559	441596,02
200	219,1	5	37,778	0,2091	0,0542	1,5774	328187,57
250	273	5,6	47,222	0,2618	0,0542	1,0062	262123,84

diameter	Λ	J (mss/m)	H_K (mss)	H_L(mss)	H_m(mss)
15	0,037106592	8578,998987	20589597,57	153375,4225	20743232,99
20	0,033662559	1735,656715	4165576,115	46176,46663	4212012,582
25	0,031341408	510,3398044	1224815,53	18363,70	1243439,226
32	0,028867061	117,3588326	281661,1982	6051,428529	287972,6267
40	0,027642635	52,51501437	126036,0345	3292,536329	129588,5708
50	0,025901152	15,01499462	36035,98709	1273,890868	37569,87796
65	0,024206154	3,806878909	9136,509381	448,6234282	9845,132809
80	0,023269134	1,637981041	3931,154498	235,8252262	4426,979724
100	0,021898393	0,410067958	984,163099	81,75648625	1325,919585
125	0,02096134	0,136863533	328,4724786	35,19348653	623,6659651
150	0,02027722	0,054242388	130,1817316	17,23580789	407,4175395
200	0,019374883	0,011750	28,20107236	5,257987768	293,4590601
250	0,018901298	0,00372588	8,942112169	2,139720925	271,0818331

Table 4 Calculation of whole desired values for all nominal diameter (continued)

diameter	N_m (kW)	A.E.C($/year)	A.F.C.($/(year * m))	A.T.F.C. ($/year)	A.T.C. ($/year)
15	16166238632	5314246794272,53	0,331	793,6732405	5314246795066,20
20	3282632006	1079083206088,54	0,432	1035,761699	1079083207124,30
25	969074360,9	318558969283,33	0,623	1496,019697	318558970779,35
32	224431466,6	73776233862,30	0,800	1919,312092	73776235781,62
40	100994852,7	33199532944,00	0,921	2211,412837	33199535155,41
50	29280084,39	9625095739,81	1,287	3089,88952	9625098829,70
65	7672804,255	2522242578,58	1,654	3970,54065	2522246549,12
80	3450166,648	1134156031,25	2,151	5162,137734	1134161193,39
100	1033355,429	339689763,33	3,159	7581,57269	339697344,90
125	486054,0699	159778124,14	4,268	10243,82092	159788367,96
150	317520,8594	104377044,51	5,076	12181,25341	104389225,76
200	228707,3185	75181813,28	6,035	14485,11602	75196298,39
250	211267,6266	69448950,56	7,544	18106,39503	69467056,96

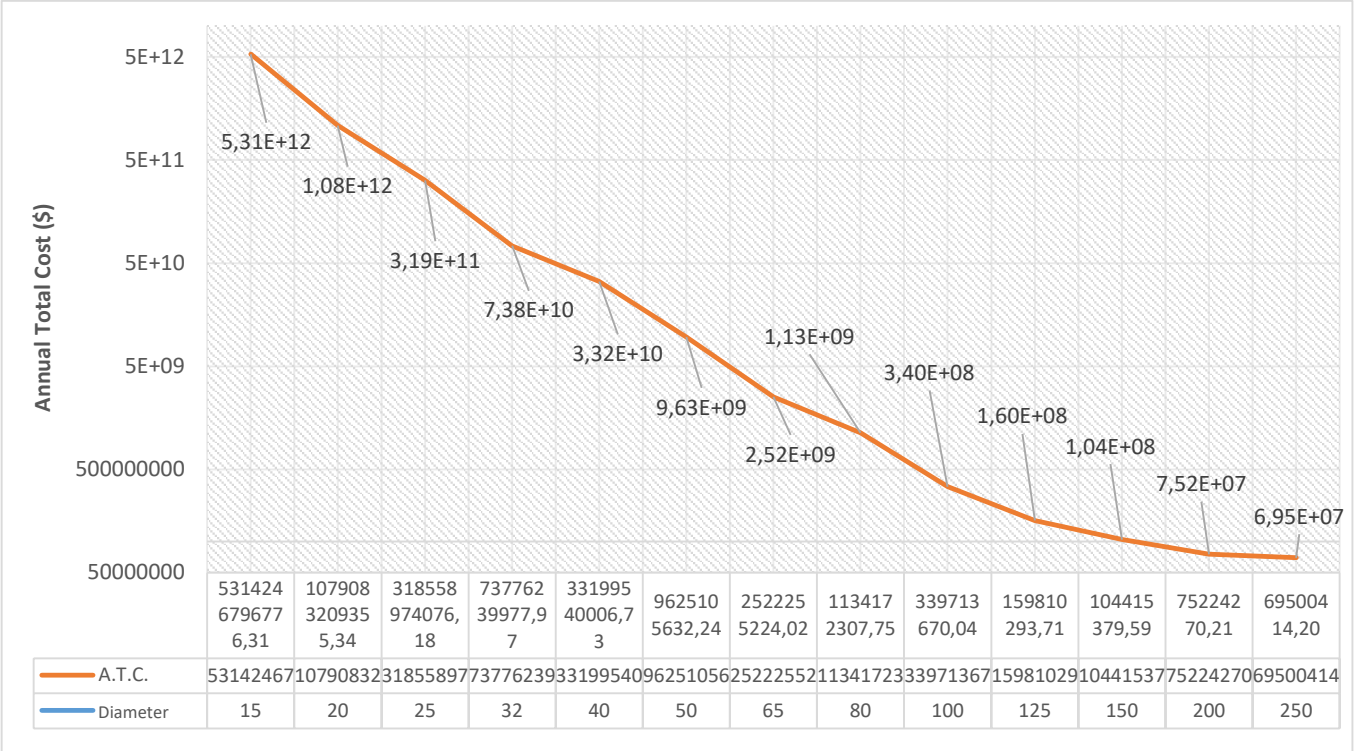

Fig.1. ATC & Diameter Chart.

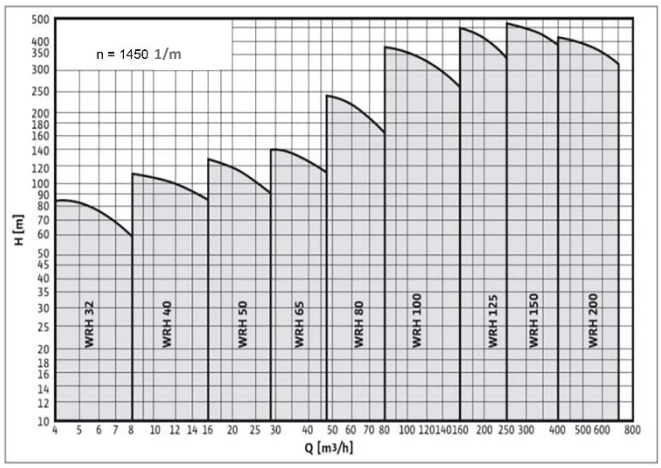

Fig. 2. Selection Table for Horizontal Step Pumps [16].

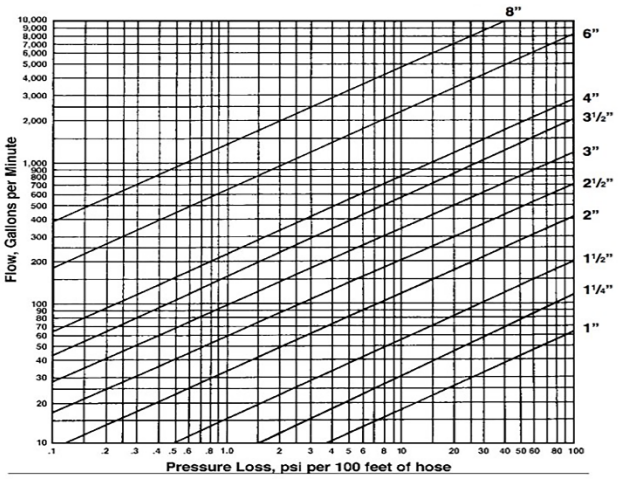

Fig.3. Volumetric Calculation Fluid Chart [11].

5. Conclusion

This approachment is intended to make possible engineers and researchers in detect cost-effective solutions for the pump select. The comparison of results of current work with other state of art works in the literature is presented in Table 1.a., Table 1.b. and Figure1. From the table it is clear that many experiment have worked on economic pump choose. As a result of the experimental work done, the loss coefficients are calculated with the aid of the determined pressure deductions taking into consideration the flow direction for the flat pipes, valves and fittings (elbows, nipples, cuffs, record, curve, reduction and TE transitional elements) that was calculated and presented in tables. When selecting a pump, the pump type, the environmental characteristics of the pump and the installation project should be considered.

For all cases insulated and uninsulated, the use of stainless steel pipes at optimum diameters allows the system to operate with minimal loss. Depending on the increase in pipe diameter, the in-pipe friction losses decrease and this reduces the pump's loss power. The diameter of the smallest of all these increases and decreases is the optimum diameter that should be preferred.

In this study, the process of transporting a certain amount of water to a certain distance has been examined. It is crucial that many criteria be evaluated at the same time in order to select the correct, appropriate and appropriate pump to be understood from the most appropriate pump selection. The environmental characteristics of the pump to be used, the type of pump and the installation project must be carefully considered when selecting a pump. The error that might happen in any of these three items may cause the inefficient operation of our pump no matter how the other parameters are.

According to Table3, to choose the ideal pipe diameter for us, all diameter values are read one by one and we get the closest values to each other. It appears here that the diameters of 150, 200 and 250 mm were determined by A.T.C. very close to each other. When the external factors such as price variability, quantity and so on are considered, they are the closest 200 and 250 mm diameters. If we consider these two diameters from the most economical point of view, 200 mm will be the ideal diameter for us. The energy required from us for this diameter value, manometric pressing pressure Hm: 239,459 m flow rate: 195 m^3/h. If you want to use one pump we can use one multi-stage full centrifugal pump of type WRH125 for 1450 pumps or these pumps can be selected in other pumps that allow WRH 80 and WRH 100 as well from Fig. 2.

References

[1] Pump life cycle costs : a guide to LCC analysis for pumping systems : executive summary, Office of Industrial Technologies, Energy Efficiency and Renewable Energy, U.S. Dept. of Energy ; [Parsippany, NJ] : Hydraulic Institute ; [Brussels, Belgium] : Europump, January 2001.

[2] P. Cooper, G Tchobanoglous - Pumpin Station Design, pp. 241-786, 2008.

[3] United States. Department of Energy, Improving Pumping System Performance: A Sourcebook for Industry, Second Edition, s, 2006, pp 6.

[4] KSB, KRT Planning Information KSB Know-how, Volume 7, 2012, pp. 15.

[5] G, Ibrahim, Chamber Of Mechanical Engineers Installation Engineering Magazine Monthly Technical Association Publication Volume: 1 Issue: 11, January 1994, pp. 11-20.

[6] Yavuz C. Atik K., "Thermo-economic Optimization of the Pipe Diameters of Hot Water Heating Systems" Electronic Journal of Machine Technologies, 8(4), 2011, pp. 53-64,

[7] Y. Zehra, S. Abdulkadir, Energy Efficiency and Applications in Centrifugal Pumps, 10:59, 2011 pp. 49.

[8] Energy Cost Referance for 2019 year database : https://www.epdk.org.tr/detay/icerik/3-0-1/tarifeler

[9] DIN 2440 Medium Serie : www.simcelik.com.tr/dokumanlar/155 212996383d4.pdf

[10] Pipe Parameters: http://www.svlele.com/piping/pipe_sizing.htm?cv=1

[11] Volumetric Flow Rate Calculation : https://inspectapedia.com/water/Water_Flow_Rate_Measurement.php

[12] Ç. Derya, "Energy Saving in Centrifu-gal Pump Systems", Sat 6: 6, 2006.

[13] Peer-review under responsibility of the scientific committee of the 72nd Conference of the Italian Thermal Machines Engineering Association 10.1016/j.egypro.08.262, 2017.

[14] P.G. Rahrig, Galvanized steel in water and water infrastructure, Mater. Perform, 2003, 42 58–60.

[15] Equipment loss coefficient value : http://www.muhendislikbilgileri.com/?Syf=15&blg=1&ncat_id=158536&pt=TABLOLAR

[16] Wilo Catalog, Selection Table for Horizontal Step Pumps, website: http://www.wilo-usa.com/fileadmin/us/USA_General/2014_Wilo_Product_Catalog.pdf

INTERNATIONAL JOURNAL OF ENGINEERING TECHNOLOGIES-IJET

Guide for Authors

The **International Journal of Engineering Technologies (IJET)** seeks to promote and disseminate knowledge of the various topics of engineering technologies. The journal aims to present to the international community important results of work in the fields of engineering such as imagining, researching, planning, creating, testing, improving, implementing, using and asking. The journal also aims to help researchers, scientists, manufacturers, institutions, world agencies, societies, etc. to keep up with new developments in theory and applications and to provide alternative engineering solutions to current.

The *International Journal of Engineering Technologies* is a quarterly published journal and operates an online submission and peer review system allowing authors to submit articles online and track their progress via its web interface. The journal aims for a publication speed of **60 days** from submission until final publication.

The coverage of IJET includes the following engineering areas, but not limited to:

All filed of engineering such as;

Chemical engineering

- Biomolecular engineering
- Materials engineering
- Molecular engineering
- Process engineering

Civil engineering

- Environmental engineering
- Geotechnical engineering
- Structural engineering
- Transport engineering
- Water resources engineering

Electrical engineering

- Computer engineering
- Electronic engineering
- Optical engineering
- Power engineering

Mechanical engineering

- Acoustical engineering
- Manufacturing engineering
- Thermal engineering
- Vehicle engineering

Systems (interdisciplinary) engineering

- Aerospace engineering
- Agricultural engineering
- Applied engineering
- Biological engineering
- Building services engineering
- Energy engineering
- Railway engineering
- Industrial engineering
- Mechatronics
- Military engineering
- Nano engineering
- Nuclear engineering
- Petroleum engineering

Types of Articles submitted should be original research papers, not previously published, in one of the following categories,

- Applicational and design studies.
- Technology development,

– Comparative case studies.

– Reviews of special topics.

– Reviews of work in progress and facilities development.

– Survey articles.

– Guest editorials for special issues.

Ethic Responsibilities

The publication of an article in peer-reviewed *"International Journal of Engineering Technologies"* is an essential building block in the development of a coherent and respected network of knowledge. It is a direct reflection of the quality of the work. Peer-reviewed articles support and embody the scientific method. It is therefore important to agree upon standards of expected ethical behavior for all parties involved in the act of publishing: the author, the journal editor, the peer reviewer, the publisher and the society of society-owned or sponsored journals.

All authors are requested to disclose any actual or potential conflict of interest including any financial, personal or other relationships with other people or organizations within three years of beginning the submitted work that could inappropriately influence, or be perceived to influence, their work.

Submission of an article implies that the work described has not been published previously that it is not under consideration for publication elsewhere. The submission should be approved by all authors and tacitly or explicitly by the responsible authorities where the work was carried out, and that, if accepted, it will not be published elsewhere in the same form, in English or in any other language, including electronically without the written consent of the copyright-holder.

Upon acceptance of an article, authors will be asked to complete a "Copyright Form". Acceptance of the agreement will ensure the widest possible dissemination of information. An e-mail will be sent to the corresponding author confirming receipt of the manuscript together with a "Copyright Form" form or a link to the online version of this agreement.

Author Rights

As a journal author, you retain rights for a large number of author uses, including use by your employing institute or company. These rights are retained and permitted without the need to obtain specific permission from *IJET.* These include:

- The right to make copies (print or electronic) of the journal article for your own personal use, including for your own classroom teaching use;
- The right to make copies and distribute copies (including via e-mail) of the journal article to research colleagues, for personal use by such colleagues for scholarly purposes;
- The right to post a pre-print version of the journal article on internet web sites including electronic pre-print servers, and to retain indefinitely such version on such servers or sites for scholarly purposes
- the right to post a revised personal version of the text of the final journal article on your personal or institutional web site or server for scholarly purposes
- The right to use the journal article or any part thereof in a printed compilation of your works, such as collected writings or lecture notes.

Article Style

Authors must strictly follow the guide for authors, or their articles may be rejected without review. Editors reserve the right to adjust the style to certain standards of uniformity. Follow Title, Authors, Affiliations, Abstract, Keywords, Introduction, Materials and Methods, Theory/Calculation, Conclusions, Acknowledgements, References order when typing articles. The corresponding author should be identified with an asterisk and footnote. Collate

acknowledgements in a separate section at the end of the article and do not include them on the title page, as a footnote to the title or otherwise.

Abstract and Keywords:

Enter an abstract of up to 250 words for all articles. This is a concise summary of the whole paper, not just the conclusions, and is understandable without reference to the rest of the paper. It should contain no citation to other published work. Include up to six keywords that describe your paper for indexing purposes.

Abbreviations and Acronyms:

Define abbreviations and acronyms the first time they are used in the text, even if they have been defined in the abstract. Abbreviations such as IEEE, SI, MKS, CGS, sc, dc, and rms do not have to be defined. Do not use abbreviations in the title unless they are unavoidable.

Text Layout for Peer Review:

Use single column layout, double spacing and wide (3 cm) margins on white paper at the peer review stage. Ensure that each new paragraph is clearly indicated. Present tables and figure legends in the text where they are related and cited. Number all pages consecutively; use 12 pt font size and standard fonts; Times New Roman, Helvetica, or Courier is preferred.

Research Papers should not exceed 12 printed pages in two-column publishing format, including figures and tables.

Technical Notes and *Letters* should not exceed 2,000 words.

Reviews should not exceed 20 printed pages in two-column publishing format, including figures and tables.

Equations:

Number equations consecutively with equation numbers in parentheses flush with the right margin, as in (1). To make equations more compact, you may use the solidus (/), the exp function, or appropriate exponents. Italicize Roman symbols for quantities and variables, but not Greek symbols. Use an dash (–) rather than a hyphen for a minus sign. Use parentheses to avoid ambiguities in denominators. Punctuate equations with commas or periods when they are part of a sentence, as in

$$C = a + b \qquad (1)$$

Symbols in your equation should be defined before the equation appears or immediately following. Use “Eq. (1)” or “equation (1),” while citing.

Figures and Tables:

All illustrations must be supplied at the correct resolution:

* Black and white and colour photos - 300 dpi

* Graphs, drawings, etc - 800 dpi preferred; 600 dpi minimum

* Combinations of photos and drawings (black and white and color) - 500 dpi

In addition to using figures in the text, upload each figure as a separate file in either .tiff or .eps format during submission, with the figure number.

Table captions should be written in the same format as figure captions; for example, “Table 1. Appearance styles.”. Tables should be referenced in the text unabbreviated as “Table 1.”

References:

Please ensure that every reference cited in the text is also present in the reference list (and viceversa). Any references cited in the abstract must be given in full. Unpublished results and personal communications are not recommended in the reference list, but may be mentioned in the text. Citation of a reference as “in press” implies that the item has been accepted for publication. Number citations consecutively in square brackets [1]. Punctuation follows the bracket [2]. Refer simply to the reference number, as in [3]. Use “Ref. [3]” or Reference [3]” at the beginning of a sentence: “Reference [3] was …”. Give all authors’ names; use “et al.” if there are six authors or more. For papers published in translated journals, first give the English citation, then the original foreign-language citation.

Books

[1] J. Clerk Maxwell*, A Treatise on Electricity and Magnetism,* 3rd ed., vol. 2. Oxford:Clarendon Press, 1892, pp.68-73.

Journals

[2] Y. Yorozu, M. Hirano, K. Oka, and Y. Tagawa, “Electron spectroscopy studies on magneto-optical media and plastic substrate interface”, *IEEE Transl. J. Magn. Japan*, vol. 2, pp. 740-741, August 1987.

Conferences

[3] Çolak I., Kabalci E., Bayindir R., and Sagiroglu S, “The design and analysis of a 5-level cascaded voltage source inverter with low THD”, *2nd PowerEng Conference*, Lisbon, pp. 575-580, 18-20 March 2009.

Reports

[4] IEEE Standard 519-1992, Recommended practices and requirements for harmonic control in electrical power systems, *The Institute of Electrical and Electronics Engineers*, 1993.

Text Layout for Accepted Papers:

A4 page margins should be margins: top = 24 mm, bottom = 24 mm, side = 15 mm. Main text should be given in two column. The column width is 87mm (3.425 in). The space between the two columns is 6 mm (0.236 in). Paragraph indentation is 3.5 mm (0.137 in). Follow the type sizes specified in Table. Position figures and tables at the tops and bottoms of columns. Avoid placing them in the middle of columns. Large figures and tables may span across both columns. Figure captions should be centred below the figures; table captions should be centred above. Avoid placing figures and tables before their first mention in the text. Use the abbreviation “Fig. 1,” even at the beginning of a sentence.

Type size (pts.)	Appearance		
	Regular	**Bold**	*Italic*
10	Authors' affiliations, Section titles, references, tables, table names, first letters in table captions,figure captions, footnotes, text subscripts, and superscripts	**Abstract**	
12	Main text, equations, Authors' names, [a]		*Subheading (1.1.)*
24	Paper title		

Submission checklist:

It is hoped that this list will be useful during the final checking of an article prior to sending it to the journal's Editor for review. Please consult this Guide for Authors for further details of any item. Ensure that the following items are present:

- ❖ One Author designated as corresponding Author:

• E-mail address

• Full postal address

• Telephone and fax numbers

- ❖ All necessary files have been uploaded

• Keywords: a minimum of 4

• All figure captions (supplied in a separate document)

• All tables (including title, description, footnotes, supplied in a separate document)

- ❖ Further considerations

• Manuscript has been "spellchecked" and "grammar-checked"

• References are in the correct format for this journal

• All references mentioned in the Reference list are cited in the text, and vice versa

• Permission has been obtained for use of copyrighted material from other sources (including the Web)

• Color figures are clearly marked as being intended for color reproduction on the Web (free of charge) and in print or to be reproduced in color on the Web (free of charge) and in black-and-white in print.

Article Template Containing Author Guidelines for Peer-Review

First Author*, Second Author**‡, Third Author***

*Department of First Author, Faculty of First Author, Affiliation of First Author, Postal address

**Department of Second Author, Faculty of First Author, Affiliation of First Author, Postal address

***Department of Third Author, Faculty of First Author, Affiliation of First Author, Postal address

(First Author Mail Address, Second Author Mail Address, Third Author Mail Address)

‡ Corresponding Author; Second Author, Postal address, Tel: +90 312 123 4567, Fax: +90 312 123 4567,corresponding@affl.edu

Received: xx.xx.xxxx Accepted:xx.xx.xxxx

Abstract- Enter an abstract of up to 250 words for all articles. This is a concise summary of the whole paper, not just the conclusions, and is understandable without reference to the rest of the paper. It should contain no citation to other published work. Include up to six keywords that describe your paper for indexing purposes. Define abbreviations and acronyms the first time they are used in the text, even if they have been defined in the abstract. Abbreviations such as IEEE, SI, MKS, CGS, sc, dc, and rms do not have to be defined. Do not use abbreviations in the title unless they are unavoidable.

Keywords- Keyword1; keyword2; keyword3; keyword4; keyword5.

2. Introduction

Authors should any word processing software that is capable to make corrections on misspelled words and grammar structure according to American or Native English. Authors may get help by from word

processor by making appeared the paragraph marks and other hidden formatting symbols. This sample article is prepared to assist authors preparing their articles to IJET.

Indent level of paragraphs should be 0.63 cm (0.24 in) in the text of article. Use single column layout, double-spacing and wide (3 cm) margins on white paper at the peer review stage. Ensure that each new paragraph is clearly indicated. Present tables and figure legends in the text where they are related and cited. Number all pages consecutively; use 12 pt font size and standard fonts; Times New Roman, Helvetica, or Courier is preferred. Indicate references by number(s) in square brackets in line with the text. The actual authors can be referred to, but the reference number(s) must always be given. Example: "..... as demonstrated [3, 6]. Barnaby and Jones [8] obtained a different result ...."

IJET accepts submissions in three styles that are defined as Research Papers, Technical Notes and Letter, and Review paper. The requirements of paper are as listed below:

- Research Papers should not exceed 12 printed pages in two-column publishing format, including figures and tables.
- Technical Notes and Letters should not exceed 2,000 words.
- Reviews should not exceed 20 printed pages in two-column publishing format, including figures and tables.

Authors are requested write equations using either any mathematical equation object inserted to word processor or using independent equation software. Symbols in your equation should be defined before the equation appears or immediately following. Use “Eq. (1)” or “equation (1),” while citing. Number equations consecutively with equation numbers in parentheses flush with the right margin, as in Eq. (1). To make equations more compact, you may use the solidus (/), the exp function, or appropriate exponents. Italicize Roman symbols for quantities and variables, but not Greek symbols. Use an dash (–) rather than a hyphen for a minus sign. Use parentheses to avoid ambiguities in denominators. Punctuate equations with commas or periods when they are part of a sentence, as in

$$C = a + b \tag{1}$$

Section titles should be written in bold style while sub section titles are italic.

3. Figures and Tables

3.1. Figure Properties

All illustrations must be supplied at the correct resolution:

- Black and white and colour photos - 300 dpi
- Graphs, drawings, etc - 800 dpi preferred; 600 dpi minimum
- Combinations of photos and drawings (black and white and colour) - 500 dpi

In addition to using figures in the text, Authors are requested to upload each figure as a separate file in either .tiff or .eps format during submission, with the figure number as Fig.1., Fig.2a and so on. Figures are cited as “Fig.1” in sentences or as “Figure 1” at the beginning of sentence and paragraphs. Explanations related to figures should be given before figure. Figures and tables should be located at the top or bottom side of paper as done in accepted article format.

Figure 1. Engineering technologies.

Table captions should be written in the same format as figure captions; for example, “Table 1. Appearance styles.”. Tables should be referenced in the text unabbreviated as “Table 1.”

Table 1. Appearance properties of accepted manuscripts

Type size (pts.)	Appearance		
	Regular	**Bold**	*Italic*
10	Authors’ affiliations, Abstract, keywords, references, tables, table names, figure captions, footnotes, text subscripts, and superscripts	**Abstract**	
12	Main text, equations, Authors’ names, Section titles		*Subheading (1.1.)*
24	Paper title		

4. Submission Process

The *International Journal of Engineering Technologies* operates an online submission and peer review system that allows authors to submit articles online and track their progress via a web interface. Articles that are prepared referring to this template should be controlled according to submission checklist given in “Guide f Authors”. Editor handles submitted articles to IJET primarily in order to control in terms of compatibility to aims and scope of Journal.

Articles passed this control are checked for grammatical and template structures. If article passes this control too, then reviewers are assigned to article and Editor gives a reference number to paper. Authors registered to online submission system can track all these phases.

Editor also informs authors about processes of submitted article by e-mail. Each author may also apply to Editor via online submission system to review papers related to their study areas. Peer review is a critical element of publication, and one of the major cornerstones of the scientific process. Peer Review serves two key functions:

- Acts as a filter: Ensures research is properly verified before being published
- Improves the quality of the research

5. Conclusion

The conclusion section should emphasize the main contribution of the article to literature. Authors may also explain why the work is important, what are the novelties or possible applications and extensions. Do not replicate the abstract or sentences given in main text as the conclusion.

Acknowledgements

Authors may acknowledge to any person, institution or department that supported to any part of study.

References

[1] J. Clerk Maxwell, *A Treatise on Electricity and Magnetism*, 3rd ed., vol. 2. Oxford:Clarendon Press, 1892, pp.68-73. (Book)

[2] H. Poor, *An Introduction to Signal Detection and Estimation*, New York: Springer-Verlag, 1985, ch. 4. (Book Chapter)

[3] Y. Yorozu, M. Hirano, K. Oka, and Y. Tagawa, "Electron spectroscopy studies on magneto-optical media and plastic substrate interface", *IEEE Transl. J. Magn. Japan*, vol. 2, pp. 740-741, August 1987. (Article)

[4] E. Kabalcı, E. Irmak, I. Çolak, "Design of an AC-DC-AC converter for wind turbines", *International Journal of Energy Research*, Wiley Interscience, DOI: 10.1002/er.1770, Vol. 36, No. 2, pp. 169-175. (Article)

[5] I. Çolak, E. Kabalci, R. Bayindir R., and S. Sagiroglu, "The design and analysis of a 5-level cascaded voltage source inverter with low THD", *2nd PowerEng Conference*, Lisbon, pp. 575-580, 18-20 March 2009. (Conference Paper)

[6] IEEE Standard 519-1992, Recommended practices and requirements for harmonic control in electrical power systems, *The Institute of Electrical and Electronics Engineers*, 1993. (Standards and Reports)

Article Template Containing Author Guidelines for Accepted Papers

First Author*, Second Author**‡, Third Author***

*Department of First Author, Faculty of First Author, Affiliation of First Author, Postal address

**Department of Second Author, Faculty of First Author, Affiliation of First Author, Postal address

***Department of Third Author, Faculty of First Author, Affiliation of First Author, Postal address

(First Author Mail Address, Second Author Mail Address, Third Author Mail Address)

‡ Corresponding Author; Second Author, Postal address, Tel: +90 312 123 4567,

Fax: +90 312 123 4567,corresponding@affl.edu

Received: xx.xx.xxxx Accepted:xx.xx.xxxx

Abstract- Enter an abstract of up to 250 words for all articles. This is a concise summary of the whole paper, not just the conclusions, and is understandable without reference to the rest of the paper. It should contain no citation to other published work. Include up to six keywords that describe your paper for indexing purposes. Define abbreviations and acronyms the first time they are used in the text, even if they have been defined in the abstract. Abbreviations such as IEEE, SI, MKS, CGS, sc, dc, and rms do not have to be defined. Do not use abbreviations in the title unless they are unavoidable.

Keywords Keyword1, keyword2, keyword3, keyword4, keyword5.

1. Introduction

Authors should any word processing software that is capable to make corrections on misspelled words and grammar structure according to American or Native English. Authors may get help by from word processor by making appeared the paragraph marks and other hidden formatting symbols. This sample article is prepared to assist authors preparing their articles to IJET.

Indent level of paragraphs should be 0.63 cm (0.24 in) in the text of article. Use single column layout, double-spacing and wide (3 cm) margins on white paper at the peer review stage. Ensure that each new paragraph is clearly indicated. Present tables and figure legends in the text where they are related and cited. Number all pages consecutively; use 12 pt font size and standard fonts; Times New Roman, Helvetica, or Courier is preferred. Indicate references by number(s) in square brackets in line with the text. The actual authors can be referred to, but the reference number(s) must always be given. Example: "..... as demonstrated [3,6]. Barnaby and Jones [8] obtained a different result ...."

IJET accepts submissions in three styles that are defined as Research Papers, Technical Notes and Letter, and Review paper. The requirements of paper are as listed below:

- Research Papers should not exceed 12 printed pages in two-column publishing format, including figures and tables.
- Technical Notes and Letters should not exceed 2,000 words.
- Reviews should not exceed 20 printed pages in two-column publishing format, including figures and tables.

Authors are requested write equations using either any mathematical equation object inserted to word processor or using independent equation software. Symbols in your equation should be defined before the equation appears or immediately following. Use “Eq. (1)” or “equation (1),” while citing. Number equations consecutively with equation numbers in parentheses flush with the right margin, as in Eq. (1). To make equations more compact, you may use the solidus (/), the exp function, or appropriate exponents. Italicize Roman symbols for quantities and variables, but not Greek symbols. Use an dash (-) rather than a hyphen for a

minus sign. Use parentheses to avoid ambiguities in denominators. Punctuate equations with commas or periods when they are part of a sentence, as in

$$C = a + b \quad (1)$$

Section titles should be written in bold style while sub section titles are italic.

6. Figures and Tables

6.1. Figure Properties

All illustrations must be supplied at the correct resolution:

- Black and white and colour photos - 300 dpi
- Graphs, drawings, etc - 800 dpi preferred; 600 dpi minimum
- Combinations of photos and drawings (black and white and colour) - 500 dpi

In addition to using figures in the text, Authors are requested to upload each figure as a separate file in either .tiff or .eps format during submission, with the figure number as Fig.1., Fig.2a and so on. Figures are cited as "Fig.1" in sentences or as "Figure 1" at the beginning of sentence and paragraphs. Explanations related to figures should be given before figure.

Fig. 1. Engineering technologies.

Figures and tables should be located at the top or bottom side of paper as done in accepted article format. Table captions should be written in the same format as figure captions; for example, "Table 1. Appearance styles.". Tables should be referenced in the text unabbreviated as "Table 1."

Table 1. Appearance properties of accepted manuscripts

Type size (pts.)	Appearance		
	Regular	**Bold**	*Italic*
10	Main text, section titles, authors' affiliations, abstract, keywords, references, tables, table names, figure captions, equations, footnotes, text subscripts, and superscripts	**Abstract-**	*Subheading (1.1.)*
12	Authors' names,		
24	Paper title		

6.2. Text Layout for Accepted Papers

A4 page margins should be margins: top = 24 mm, bottom = 24 mm, side = 15 mm. The column width is 87mm (3.425 in). The space between the two columns is 6 mm (0.236 in). Paragraph indentation is 3.5 mm (0.137 in). Follow the type sizes specified in Table. Position figures and tables at the tops and bottoms of columns. Avoid placing them in the middle of columns. Large figures and tables may span across both columns. Figure captions should be centred below the figures; table captions should be centred above. Avoid placing figures and tables before their first mention in the text. Use the abbreviation "Fig. 1," even at the beginning of a sentence.

7. Submission Process

The International Journal of Engineering Technologies operates an online submission and peer review system that allows authors to submit articles online and track their progress via a web interface. Articles that are prepared referring to this template should be controlled according to submission checklist given in "Guide f Authors". Editor handles submitted articles to IJET primarily in order to control in terms of compatibility to aims and scope of Journal. Articles passed this control are checked for grammatical and template structures. If article passes this control too, then reviewers are assigned to article and Editor gives a reference number to paper. Authors registered to online submission system can track all these phases. Editor also informs authors about processes of submitted article by e-mail. Each author may also apply to Editor via online

submission system to review papers related to their study areas. Peer review is a critical element of publication, and one of the major cornerstones of the scientific process. Peer Review serves two key functions:

- Acts as a filter: Ensures research is properly verified before being published
- Improves the quality of the research

8. Conclusion

The conclusion section should emphasize the main contribution of the article to literature. Authors may also explain why the work is important, what are the novelties or possible applications and extensions. Do not replicate the abstract or sentences given in main text as the conclusion.

Acknowledgements

Authors may acknowledge to any person, institution or department that supported to any part of study.

References

[7] J. Clerk Maxwell, A Treatise on Electricity and Magnetism, 3rd ed., vol. 2. Oxford:Clarendon Press, 1892, pp.68-73. (Book)

[8] H. Poor, An Introduction to Signal Detection and Estimation, New York: Springer-Verlag, 1985, ch. 4. (Book Chapter)

[9] Y. Yorozu, M. Hirano, K. Oka, and Y. Tagawa, "Electron spectroscopy studies on magneto-optical media and plastic substrate interface", IEEE Transl. J. Magn. Japan, vol. 2, pp. 740-741, August 1987. (Article)

[10] E. Kabalcı, E. Irmak, I. Çolak, "Design of an AC-DC-AC converter for wind turbines", International Journal of Energy Research, Wiley Interscience, DOI: 10.1002/er.1770, Vol. 36, No. 2, pp. 169-175. (Article)

[11] I. Çolak, E. Kabalci, R. Bayindir R., and S. Sagiroglu, "The design and analysis of a 5-level cascaded voltage source inverter with low THD", 2nd PowerEng Conference, Lisbon, pp. 575-580, 18-20 March 2009. (Conference Paper)

[12] IEEE Standard 519-1992, Recommended practices and requirements for harmonic control in electrical power systems, The Institute of Electrical and Electronics Engineers, 1993. (Standards and Reports)

INTERNATIONAL JOURNAL OF ENGINEERING TECHNOLOGIES (IJET)
COPYRIGHT AND CONSENT FORM

This form is used for article accepted to be published by the IJET. Please read the form carefully and keep a copy for your files.

TITLE OF ARTICLE (hereinafter, "The Article"):

……..…….....……

……..…….....……

……...……...……

LIST OF AUTHORS:

……..……...…..……

……..…….....……

……...……...……

CORRESPONDING AUTHOR'S ("The Author") NAME, ADDRESS, INSTITUTE AND EMAIL:

……...……

……..…….....……

……...……...……..…

COPYRIGHT TRANSFER

The undersigned hereby transfers the copyright of the submitted article to International Journal of Engineering Technologies (the "IJET"). The Author declares that the contribution and work is original, and he/she is authorized by all authors and/or grant-funding agency to sign the copyright form. Author hereby assigns all including but not limited to the rights to publish, distribute, reprints, translates, electronic and published derivates in various arrangements or any other versions in full or abridged forms to IJET. IJET holds the copyright of Article in its own name.

Author(s) retain all rights to use author copy in his/her educational activities, own websites, institutional and/or funder's web sites by providing full citation to final version published in IJET. The full citation is provided including Authors list, title of the article, volume and issue number, and page number or using a link to the article in IJET web site. Author(s) have the right to transmit, print and share the first submitted copies with colleagues. Author(s) can use the final published article for his/her own professional positions, career or qualifications by citing to the IJET publication.

Once the copyright form is signed, any changes about the author names or order of the authors listed above are not accepted by IJET.

Authorized/Corresponding Author **Date/ Signature**